Studying Impacts of Microwave-Assisted Crushing of Kimberlite Ore by Analysing Size and Energy Consumption

Azlan Aslam

Department of Mining and Materials Engineering
McGill University, Montreal, Canada

December 2021

A thesis submitted to McGill University in partial fulfillment
of the requirements of the degree of
Master of Engineering

Abstract

The comminution stage in mineral processing consumes around 30% to 70% of the energy used in mining. Tonnes of excavated and mined material yield only a small quantity of diamonds in diamond mining and processing. Furthermore, out of this small recovery of diamonds, some diamonds are lost as fine tailings, contributing to an economic loss. In addition to this, in diamond processing, some coarse tailings are generally routed back for recrushing process to achieve better liberation of diamonds. However, this process sometimes causes the diamonds to break, and due to the size reduction, the value of the diamonds is reduced.

In the last few decades, research efforts have been put to reduce energy consumption by adopting preheating (pre-treatment) measures before the comminution stage. In this regard, microwave-assisted comminution has shown the potential of rock strength reduction, which ultimately can pave the way for energy reduction in comminution. However, there is not much work done on the effect of microwave irradiations on ore loss and product critical sizes after the crushing.

This research focuses on the effect of microwave irradiation on kimberlite rocks which constitute a significant source of diamonds. The effect of microwave radiation is analyzed by considering the influencing parameters like microwave power and input energy (exposure time) on particulate samples while keeping the mass of samples and distance from the antenna (horn) of microwave constant.

The 500 g particulate samples of kimberlite rocks were treated using a single-mode 15 kW power output capacity microwave at 2.45 GHz frequency. The microwave treated and untreated samples were then crushed with the help of a single roll crusher to compare the effect on specific comminution energy (E_{cs}). The crushing of samples was followed by screening to analyze the impact of microwave irradiations on the particle size distribution and critical product sizes (d_{50} and d_{80}) after crushing.

The results of this research indicate that microwaves impact kimberlite samples in terms of product size, ore loss, and specific comminution energy. Microwaves have positive as well as negative effects on product size and ore loss. The positive effect was seen, under certain experimental conditions, in terms of increased d_{50} and d_{80} of the product of crushing as well as in reducing ore

loss. However, in certain experimental conditions, the production of fines was increased, which depicted the negative impacts of microwaves as this increased the ore loss. In terms of specific comminution energy (E_{cs}), improvement was observed in reducing E_{cs} of treated kimberlite samples compared to non-treated samples. The increase in product mean sizes (d_{50} and d_{80}) leads to coarse size diamond recovery and cost-effective waste management.

In the future, this research can pave the way to study the effect of microwaves on dense media separation of crushed ore products and the effect of microwaves on breakage functions. All these present and future recommended studies can be combined to make an optimized multi-variable microwave-assisted processing system which can further help to study the cost-effectiveness of microwaves application in the kimberlite processing.

Résumé

L'étape de broyage dans le traitement des minéraux consomme environ 30 à 70 % de l'énergie utilisée dans l'exploitation minière. Des tonnes de matériaux excavés et extraits ne produisent qu'une petite quantité de diamants dans l'extraction et le traitement des diamants. De plus, sur cette petite récupération de diamants, certains diamants sont perdus sous forme de résidus fins, contribuant à une perte économique. En plus de cela, dans le traitement des diamants, certains résidus grossiers sont généralement réacheminés vers un processus de rebroyage afin d'obtenir une meilleure libération des diamants. Cependant, ce processus provoque parfois la rupture des diamants et, en raison de la réduction de la taille, la valeur des diamants est réduite.

Au cours des dernières décennies, des efforts de recherche ont été déployés pour réduire la consommation d'énergie en adoptant des mesures de préchauffage (pré-traitement) avant l'étape de broyage. À cet égard, la fragmentation assistée par micro-ondes a montré le potentiel de réduction de la résistance de la roche, ce qui peut finalement ouvrir la voie à une réduction de l'énergie de la fragmentation. Cependant, il n'y a pas beaucoup de travaux sur l'effet des irradiations par micro-ondes sur la perte de minerai et les tailles critiques du produit après le concassage.

Cette recherche se concentre sur l'effet de l'irradiation par micro-ondes sur les roches kimberlitiques qui constituent une source importante de diamants. L'effet du rayonnement micro-ondes est analysé en considérant les paramètres d'influence tels que la puissance micro-ondes et l'énergie d'entrée (temps d'exposition) sur les échantillons de particules tout en maintenant la masse des échantillons et la distance par rapport à l'antenne des micro-ondes constantes.

Les échantillons de 500 g de particules de roches kimberlitiques ont été traités à l'aide d'un micro-onde monomode d'une puissance de sortie de 15 kW à une fréquence de 2,45 GHz. Les échantillons traités aux micro-ondes et non traités ont ensuite été broyés à l'aide d'un seul broyeur à rouleaux pour comparer l'effet sur l'énergie de fragmentation spécifique (E_{cs}). Le broyage des échantillons a été suivi d'un criblage pour analyser l'impact des irradiations micro-ondes sur la distribution granulométrique et les tailles critiques des produits (d_{50} et d_{80}) après broyage.

Les résultats de cette recherche indiquent que les micro-ondes ont un impact sur les échantillons de kimberlite en termes de taille du produit, de perte de minerai et d'énergie de fragmentation

spécifique. Les micro-ondes ont des effets positifs et négatifs sur la taille du produit et la perte de minerai. L'effet positif a été observé, dans certaines conditions expérimentales, en termes d'augmentation de d_{50} et d_{80} du produit de concassage ainsi qu'en termes de réduction des pertes de minerai. Cependant, dans certaines conditions expérimentales, la production de fines a été augmentée, ce qui a représenté les impacts négatifs des micro-ondes car cela a augmenté la perte de minerai. En termes d'énergie de fragmentation spécifique (E_{cs}), une amélioration a été observée dans la réduction des E_{cs} des échantillons de kimberlite traités par rapport aux échantillons non traités.

À l'avenir, cette recherche peut ouvrir la voie à l'étude de l'effet des micro-ondes sur la séparation en milieu dense des produits de minerai concassé et de l'effet des micro-ondes sur les fonctions de rupture. Toutes ces études recommandées présentes et futures peuvent être combinées pour créer un système de traitement assisté par micro-ondes multivariable optimisé qui peut en outre aider à étudier la rentabilité de l'application des micro-ondes dans le système de traitement de la kimberlite.

Acknowledgments

First, I would like to thank Allah for blessing me with the strength and courage required to complete this thesis and research work.

I want to express my sincere gratitude to my supervisor Professor Agus P. Sasmito, and my co-supervisor, Professor Ferri Hassani, for their constant guidance, support, and supervision throughout this research work. I would also like to thank Amir Arash Rafiei and Muhammad Rasyid for assisting me and having thoughtful discussions throughout my research work. I would also like to thank Professor Ali Ghoreishi-Madiseh from the University of British Columbia for his discussions and guidance. Also, I would like to express my gratitude to the Government of Pakistan, who assisted me financially, which allowed me to pursue my studies at this institution.

The completion of this work would not have been possible without the support of my family. I greatly thank my sister, Ayesha Hussain, and my cousin, Iftikhar Hussain, their kids, Essa and Anayah, who kept me sane through the tough conditions of the pandemic and made my stay in Canada a comfortable experience. Last but not least, I would like to express my gratitude to my wife, Zaneera Azlan, for her encouragement, assistance and all the sacrifices she has made for me, and my son, Ashar Azlan, for always helping me destress with his giggles.

To my parents,

For teaching me the importance of hard work, honesty, integrity and perseverance.
May their souls rest in peace.

Contributions to Original Knowledge

This thesis considers the previous research work made in the field of impacts of microwaves on rock strength and comminution. This thesis aims to study the effects of single-mode microwave irradiations on kimberlite rocks by analyzing the parameters like product critical sizes and specific energy consumption during crushing. This thesis presents a method of determining the impacts of microwaves on ore loss, critical sizes (d_{50} and d_{80}) and circulating load using particle size distribution models. Moreover, the effects of microwave treatment on specific comminution energy during crushing are determined by analytical methods for energy calculations. This research can be employed for future investigations of the effects of microwaves on other rock types. Moreover, this knowledge of the effects of microwaves on PSD and energy can be combined with more future studies, like microwaves effect on dense media separation etc., to determine the effects of microwaves on all downstream processing operations, which can help in making feasible plans for practical application of microwaves.

Table of Contents

List of Figures

List of Tables

Nomenclature

E_{cs}	Specific comminution energy	C_p	Specific heat capacity
d_{50}	Fraction of particles < 50%	E	Electric field
d_{80}	Fraction of particles < 80%	B	Magnetic field
W_i	Work index	μ_o	Permeability of free space
P_1	Product size (required)	ε	Electrical permittivity
G	Grindability of the ore	εr	Relative permittivity
P	Product 80 % passing size/Power Density	ε0	Permittivity of free space (ε0 = 8.86×10^{-12})
F	Feed 80% passing size	ρ_c	Charge density
W	Energy required for grinding	J	Current per unit area
X	Particle size for GGS and RR model	*t* or t	Time
K	Size parameter for GGS model	ε”	Permittivity loss factor
	Distribution coefficient for GGS model	ε’	Dielectric permittivity constant
b	Size parameter for RR model	μ'	Dielectric permeability constant
n	Distribution parameter for RR model	μ''	Permeability loss factor
tan δ	Loss tangent	σ	Electrical conductivity
ρ	Density	f	Frequency
T	Temperature	W_p	% of material passing
T_{eq}	Temperature at equilibrium	W_r	% of material retained
m	Mass	R^2	R-squared

Abbreviation

MW	Microwaves
DNA	Deoxyribonucleic Acid
HK	Hypabyssal Kimberlite
VK	Volcaniclastic Kimberlite
TK	Tuffistic Kimberlite
HBHM	Hydraulic Borehole Mining
MAC	Microwave Assisted Comminution
ROM	Run Off Mine
HPGR	High Pressure Grinding Rollers
HMS	Heavy Media Separation
GGS	Gates-Gaudin-Schuhmann
RR	Rosin Rammler
UCS	Unconfined Compressive Strength
BTS	Brazilian Tensile Strength
PLS	Point Load Strength
BWI	Bond Work Index
XRD	X-Ray Diffraction
SC	Size Class
SEM	Scanning Electron Microscopy
TAL	Thermally Assisted Liberation
FLIR	Forward Looking Infrared
CV	Coefficient of Variance

1. Introduction

The increase in mining and production of minerals by mining companies is generally associated with rapid growth and industrialization (Dutta et al., 2016). The mining industry is a starting point of a critical value chain. As the industrial world today increasingly relies on minerals and materials used for energy production and transmission, machinery and construction, vehicle manufacturing and fuel, computers and other electronics, healthcare and food production and even space ventures, the need of the hour is to indulge in mining and processing of these minerals in more efficient, innovating and environmentally viable way.

The increase in demand for various minerals, materials, and elements in industries also resulted in exploring and synthesizing many new materials. Apart from discovery, much research is undergoing to bring into use some of the materials like diamonds. Diamonds are one of the hardest and expensive gemstones, which was considered only as a symbol of wealth in the past. However, at present, it has found its way into the industry due to its several remarkable properties.

1.1 Introduction to Diamonds and Kimberlite

1.1.1 Diamonds

Diamonds are formed at a depth of around 150 km beneath the earth's surface in the upper mantle due to the transformation of carbon (graphite) under high temperature and pressure. The pressure range of 40-60 kBar and temperature range of around 1000-1200 ºC results in the diamond formation. The first significant discovery of diamonds recorded in history was in India around 2700 years ago (Erlich & Dan Hausel, 2002). Its journey started as an expensive gemstone that was known as a symbol of wealth. Later in 1800, a series of discoveries were made in Africa, which boomed the mining and processing of diamonds.

Apart from many valuable minerals like copper, gold etc., diamonds have been among the top expensive stones, and their value has risen for the past few centuries. Now, diamond has started creeping into the industry and is used to make chemical and biological sensors, DNA and protein chips and can be used in making electrodes for electrolytic reactions. This increase in the use of

diamonds is due to their exceptional properties, and a few of the properties are listed below (Pierson, 1993):

1. Diamonds have the highest thermal conductivity at room temperature, which is five times that of copper.
2. It is by far the hardest known material.
3. It has exceptionally high strength and rigidity.
4. It is ideal optical material capable of transmitting light from far-infrared to ultraviolet.
5. Its semiconductor properties are remarkable, with dielectric constant value half of that of silicon

These remarkable properties of diamonds have encouraged researchers to put efforts into synthesizing them. Now, many different synthetic diamonds are available, which are produced by converting graphite (carbon) into diamonds using different pressure and temperature conditions.

1.1.2 Kimberlite: Source of Diamonds

The formation of diamonds takes place at very high pressures and temperatures. These extreme geological conditions also result in the formation of magma in the upper mantle, which rapidly expands and moves upwards while taking along the precious stones called diamonds and other minerals and rock fragments. When this mixture reaches the earth's surface, it forms a particular underground structure (pipes) which is shaped like a 'carrot.' When this magma cools down, it

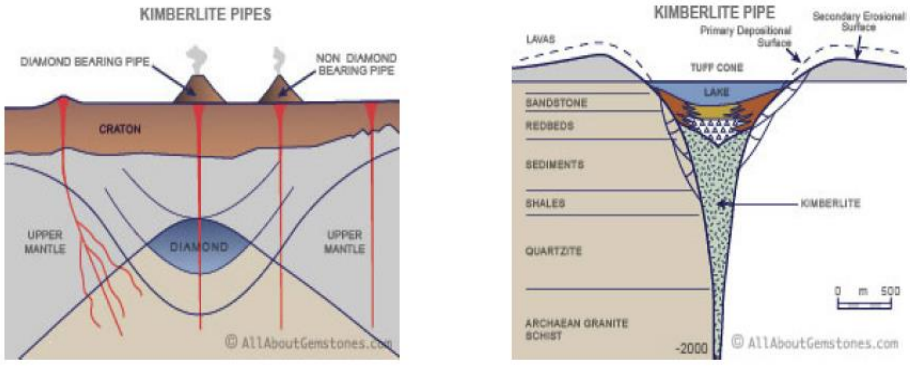

Figure 1-1 Kimberlitic pipe formation (Source: www.allaboutgemstones.com)

hardens and forms a rock called ‘Kimberlite.’ Thus, the magmatic pipes formed are known as ‘Kimberlite pipes’ (Harlow, 1998), as shown in Figure 1-1.

Kimberlite is a diverse and complex hybrid igneous rock, one of the significant sources and host rocks of diamonds. Although lamproites and placer deposits are also considered the critical sources of diamonds, kimberlites are considered the primary source of diamonds. They were first discovered in the South African region of Kimberley, due to which this rock got the name of kimberlite. Kimberlites are mainly composed of minerals like olivine ($(Mg, Fe)_2SiO_4$), phlogopite ($KMg_3(AlSi_3O_{10})(OH)_2$) and serpentine ($Mg_3Si_2O_5(OH)_4$), but these minerals vary in terms of weight percentage (Morkel, 2006).

Kimberlites have been divided into different groups based on their composition. For example, Wilson and Anhaeusser proposed classification into two groups: Olivine rich Kimberlite (< 5% mica) and Micaceous Kimberlite (> 50% mica) (Wilson & Anhaeusser, 1998). There have been some other classifications as well by different authors. Nevertheless, the classification of prime importance to this study is based on zones and emplacement mechanisms. The classification as mentioned consists of three types of Kimberlite; Coherent Kimberlite (Hypabyssal Kimberlite (HK)), Volcaniclastic Kimberlite (VK) and Tuffisitic Kimberlite (TK). Hypabyssal Kimberlite (HK) will be studied in this research.

1.2 Mine to Mill Processes of Kimberlite

The exploration process of kimberlite is an expensive process with a very low probability of success. Nevertheless, it is estimated that a small number of kimberlite pipes become economically feasible to be mined because of the low quantity of diamonds present in the kimberlite pipes. Mostly, the mining of kimberlite deposits begins with standard open pit mining methods. However, as the diamond quantity in the deposits is deficient, considerable material must be removed to recover that small quantity of diamonds. This open-pit mining then leads to underground mining in order to recover the diamonds present in greater depths. This underground mining can be costly because of higher capital and operating costs. Recently, a new technique, Hydraulic Borehole Mining (HBHM), has been under study at Merlin Diamonds in the Northern Territory of Australia, which is considered economically feasible to mine diamondiferous deposits not accessible before.

This technology uses a water jet cutting tool and a downhole slurry pumping system (Boone Beck, 2016).

After mining, the next significant step in the production of minerals is processing. The processing of minerals is done in order to liberate valuable minerals from the gangue. The minerals processing can be categorized into two main stages: comminution/liberation and concentration/separation (Maurice, N.; Kenneth, 2003). In the comminution part of mineral processing, the particles undergo a series of crushing and grinding stages to reduce the particle size, which helps to liberate the valuable minerals. In the concentration stage, the valuable minerals are separated. It is estimated that comminution accounts for 60%-75% of total energy consumption (Norgate & Haque, 2010). The main bulk of this energy is used during the grinding process as a last stage of comminution.

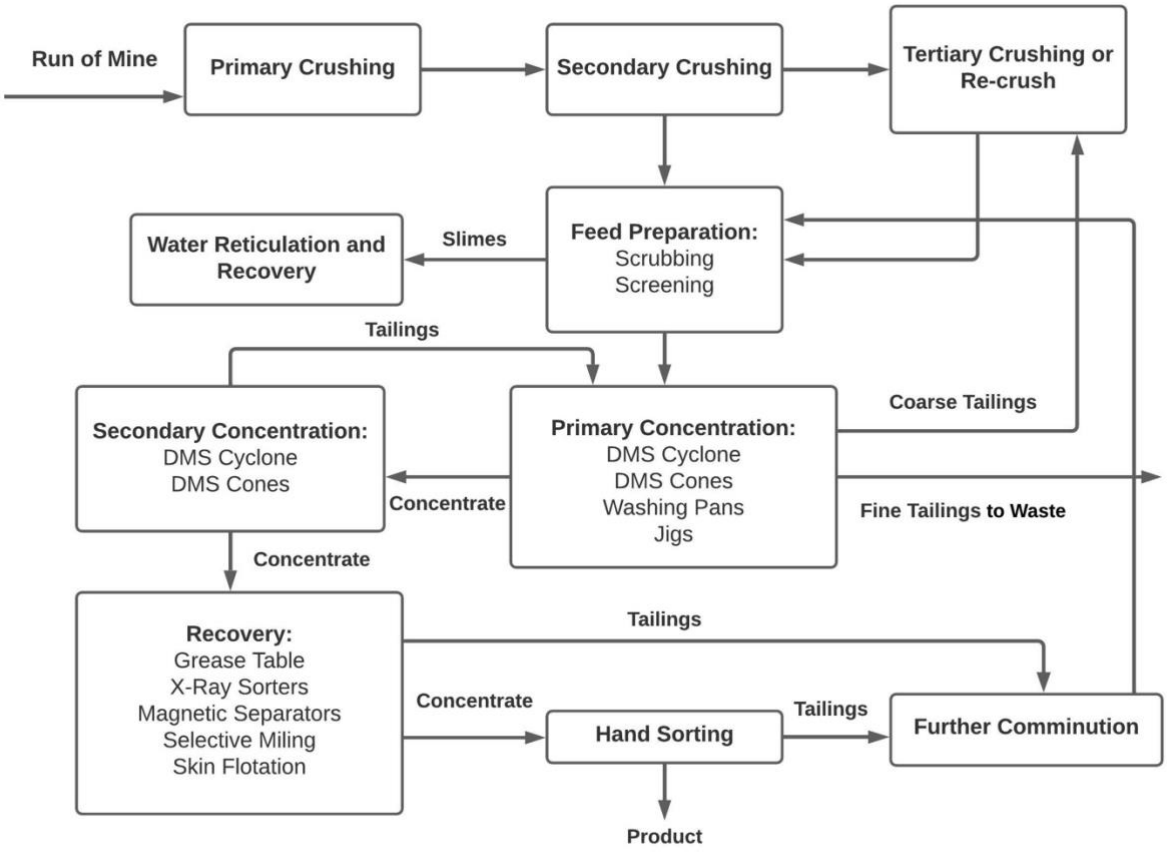

Figure 1-2 Diamond extraction flowsheet (Hodgson, 1981)

In diamond processing, all the processing steps are undertaken to achieve an optimum compromise between reducing the ore to the size at which the separation can be done and minimizing the probability of diamond breakage. The crushing of kimberlite (diamond-bearing host rock), like any other mineral, is done in several stages. The general processes involved in extracting diamonds are shown in Figure 1-2 (Hodgson, 1981). So, the processing of diamonds also consumes much energy during all the stages, as mentioned in the above paragraph for other minerals. Moreover, to ensure better recovery of intermediate and smaller size diamonds, the recrushing of the coarse tailing is done, which sometimes leads to diamond breakage.

1.3 Heating Ore prior to Comminution

The high energy demands during the comminution of ores paved the way for research of pre-treatment of ores prior to comminution. In the 1920s, the effects of heating ores before crushing were analyzed (Yates, 1918) (Holman, 1926). The research work on heating ore was based on the fact that heating can cause minerals inside the rock to expand thermally. As the minerals have different thermal expansion coefficients, thermal stress is caused along the mineral grain boundaries. These thermal stresses will induce micro-cracks along the mineral grain boundaries improving the liberation and reducing the energy consumption during crushing and grinding. Later, a more efficient way of heating the ores was introduced using microwave energy, named Microwave-Assisted Comminution (MAC).

1.4 Objectives of the Study

During the processing of diamonds, few challenges arise which need to be addressed. These challenges are:

1. Potential for physical damage on the diamond because of over crushing.
2. Losing a fraction of fine ore that is not capable of being processed by dense media separation.
3. Increase in the production rate of coarse diamond due to its higher economic value as compared to fine diamond.
4. An increase in the mean size of process reject, which results in bringing down the high cost of waste management linked with fine size fraction.

5. Energy consumption of crushing process.

This research aims to study the impact of microwave irradiations on the crushing of kimberlite (diamond host rock), considering the above challenges. The objectives of this study are:

1. Increasing the product critical size (d_{50} and d_{80}) of crusher product to make a balance among minimizing the over-crushing of diamond particles (done on particles greater than 6 mm, also called as circulating load), increasing coarse diamond production and reducing the fraction of fine particles (particles less than 1 mm) that cannot be processed by dense media separation.
2. Reducing the narrowness of crusher product size distribution.
3. Reducing the fraction of very fine waste (particles less than 300 µm) that needs more waste management cost compared to a comparatively coarser waste fraction.
4. Reducing the comminution energy consumption, E_{cs}.

1.5 Structure of Thesis

This thesis is divided into five chapters, and they are outlined below:

Chapter 1. Introduction: The first chapter introduces diamonds and kimberlites, followed by a brief description of different processes involved in mining and processing kimberlite. It also gives a brief introduction to the concept of pre-treatment of ore prior to comminution.

Chapter 2. Literature Review: This chapter throws some light on the previous work being done on microwave-assisted comminution. It also explains the concepts of microwave heating and its effect on minerals. It also reviews different research work carried out to study the effect of microwaves on ore strength reduction.

Chapter 3. Methodology and Experimental Setup: This chapter explains the materials and experimental setup used to conduct the research. It also explains the methodology which is followed for this research work.

Chapter 4. Results and Discussion: The results which are achieved keeping in view the objectives are presented in this chapter. The result data obtained from the research is also compared with published work.

Chapter 5. Conclusions and Future Work: The significant conclusions of the study done in this thesis are presented in this chapter with a few suggestions and a way forward in this research work.

2. Literature Review

This chapter provides an overview of different stages and mechanisms of comminution and processing of minerals. It also presents the research work done in the past in terms of the impacts of microwave heating on minerals.

2.1 Mineral Processing

2.1.1 Introduction

The rapid growth of industrialization has increased the demand for minerals. The minerals are basically naturally occurring metallic compounds such as oxides and sulphides of metals (Swapan K. Haldar, 2018). They are homogenous inorganic substances with unique chemical compositions and atomic structures. Minerals can have the same chemical composition but possess different physical properties based on their crystal structure (Barry A. Wills & Finch, 2016b). For example, graphite and diamond are composed of carbon atoms, but their properties differ due to the arrangement of carbon in their structure. The different minerals then combine to form rocks (Metso, Sandgren et al., 2015) which are usually heterogenous in their composition. When these rocks have a high concentration of valuable minerals with high economic value, they are categorized as ores. The ores can be metallic and non-metallic in nature. The mining and processing of these ores result in the extraction of valuable minerals.

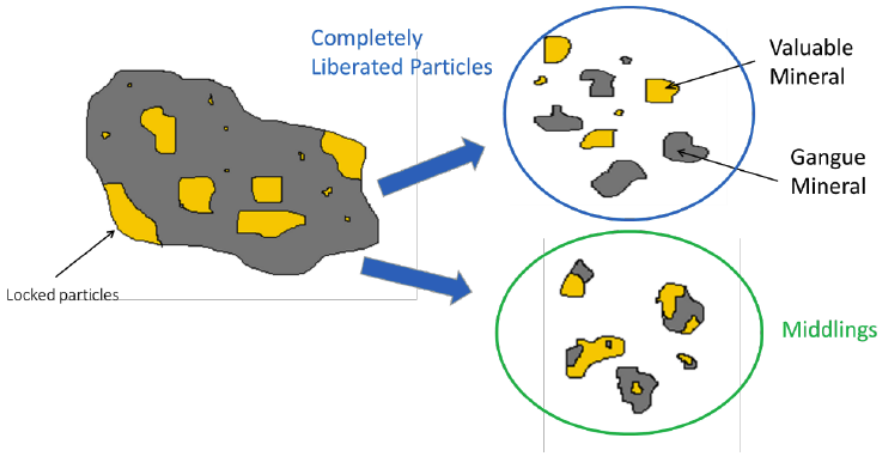

Figure 2-1 Schematic of particle liberation (Mita, 2018)

The processing of mineral ores aims to separate the valuable metallic and non-metallic minerals from non-valuable gangue. This objective is achieved in two principal stages: liberation by size reduction (Figure 2-1) and separation/concentration of valued minerals from the waste/gangue (Barry A. Wills & Finch, 2016a). The mechanical breakage of rocks into a smaller size is called comminution (T. J. Napier-Munn et al., 1996) and is usually carried out in several stages involving crushing and grinding. The main aim of comminution is to unlock the particles at the coarsest possible size. Then, in the concentration stage, the valuable mineral is separated from the gangue/waste material. This separation is achieved through different techniques, including gravity separation, magnetic separation, or froth flotation.

2.1.2 Processing of Kimberlite

The processing of Kimberlite for the extraction of diamonds varies from mine to mine but generally follows the same steps as any other minerals. The processing of kimberlite done by De Beers Group is discussed in this section. The processing begins by sending Run of Mine (ROM) feed having a size of around 200 mm for crushing, which involves primary and secondary crushing

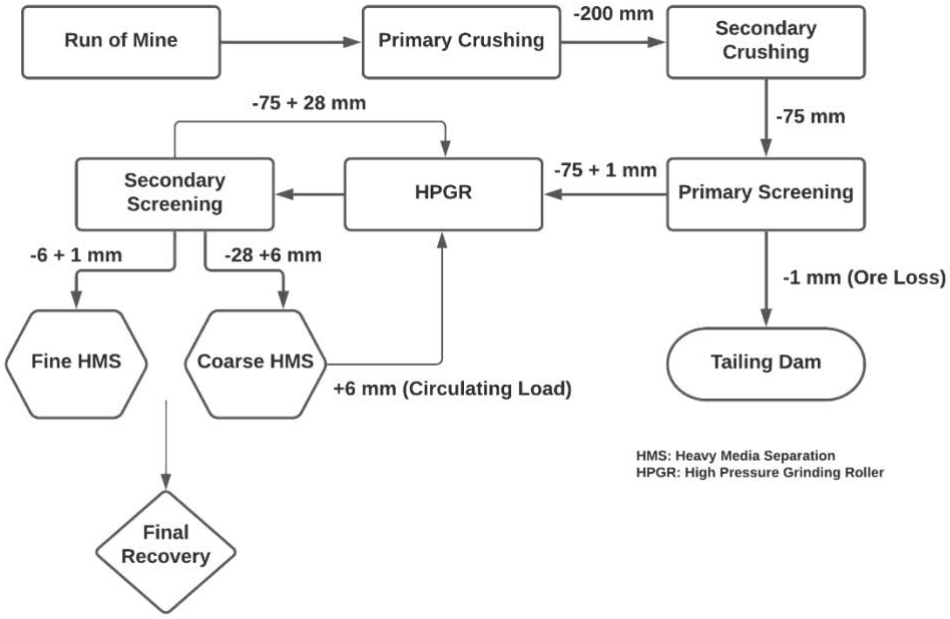

Figure 2-2 Simplified De Beers Group diamond processing flowsheet

and screening which reduces the product size down to 75 mm. After secondary crushing, the material is sent to High Pressure Grinding Rollers (HPGR), which further reduces the product's size to 28 mm. Following the comminution, the concentration stage can be divided into two stages. The primary concentration, which involves the Heavy Media Separation (HMS) procedure, also takes two steps. Firstly, the particles with a size of -28 + 6 mm are sent to the coarse HMS section, and the particles with a size of -6 + 1 mm are sent to the fine HMS section. This is followed by secondary concentration and recovery of diamonds by separating them from the gangue using different sorting techniques. Further, the processing's fines (-1 mm) are sent to tailing dams as waste as the size is very small to recover any valuable product. A point to be noted is that after the coarse HMS separation, the particles of size greater than 6 mm are sent back to HPGR for recrushing to give another chance for diamond liberation before discarding them as a waste product. This recrushing sometimes can cause damage to diamonds which can ultimately become less valuable due to their smaller size. A simplified flow chart of kimberlite processing can be seen in Figure 2-2.

2.2 Comminution

Comminution is the process of mechanical breakage of rocks or size reduction of rocks to unlock or liberate the tightly locked mineral inside an ore (Vorster, 2001). This step takes place during the mineral processing and helps in increasing the productivity of the concentration stage. Comminution involves the use of crushing units, tumbling and stirred mills, grinding mills, and screens for sizing the product (Vorster, 2001). All these units help reduce the size of the product, with the grinding operation being the last and most vital step (B. A. Wills, 1990).

It is reported that comminution is a very high energy-intensive operation and consumes up to 70 % of the energy used in mining (Nadolski et al., 2014). A significant portion of this energy consumption takes place in grinding units (T. Napier-Munn, 2015). It is estimated that out of this high energy consumption, only 1-2% is used for breakage (Fuerstenau & Abouzeid, 2002). This high energy consumption increases the operational cost of the whole processing operation. If this energy consumption can be brought down, this can significantly reduce the operational cost. Considering this aspect, much research has been put into reducing the energy consumption by pre-treatment of ore either by conventional heating or microwave treatments.

2.2.1 Breakage Mechanism

Minerals primarily exist in crystalline forms with atoms arranged in proper three-dimensional arrays. The bonds between these atoms are effective for a small distance and can be broken using compressive or tensile force (Barry A. Wills & Finch, 2016a). Different minerals are distributed as grains of various sizes inside the rocks, resulting in different internal stresses on the application of load. Although it is said that rocks exist in brittle form, they can store energy which shows they have an elastic nature (Barry A. Wills & Finch, 2016a). In order to break the rocks, first, this stored energy is lost, which initiates the process of fracturing. Second, as the rocks have different minerals with different properties, the mineral boundaries behave as small naturally occurring flaws. When the energy applied exceeds the fracture energy, these natural flaws will move along the weakest planes resulting in the ultimate breakage of the particles.

One of the researchers named King explains the fracturing of particles, which states that three different modes/patterns of fracture occur when a single particle breaks (King, 2001). The first pattern is shattering, which takes place due to a brisk application of compressive stress. The product size produced by this fracture mode is in a wide range, as shown in Figure 2-3. The breakage takes place in series of steps of fracturing until all the energy available for fracture is diminished.

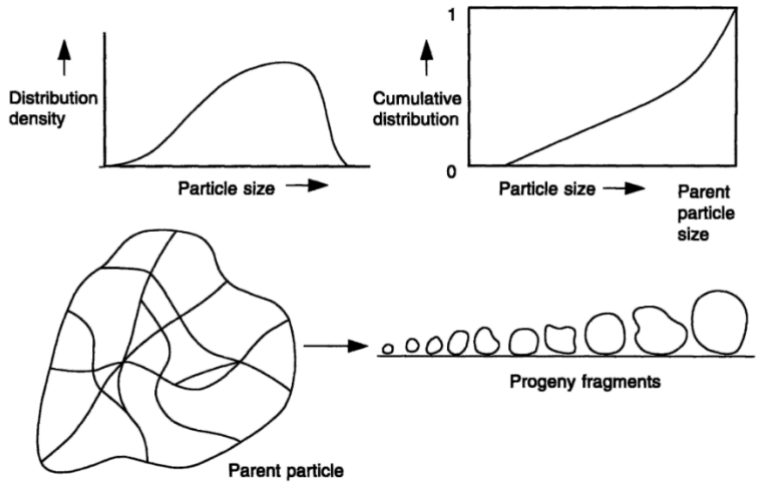

Figure 2-3 Shattering fracture mechanism with particle size distribution (King, 2001)

The second mode of fracture is cleavage, which occurs when the original material already has some preferred surfaces where fracture can occur. The product size range in such a fracture mechanism is usually narrow and sometimes bimodal, as shown in Figure 2-4.

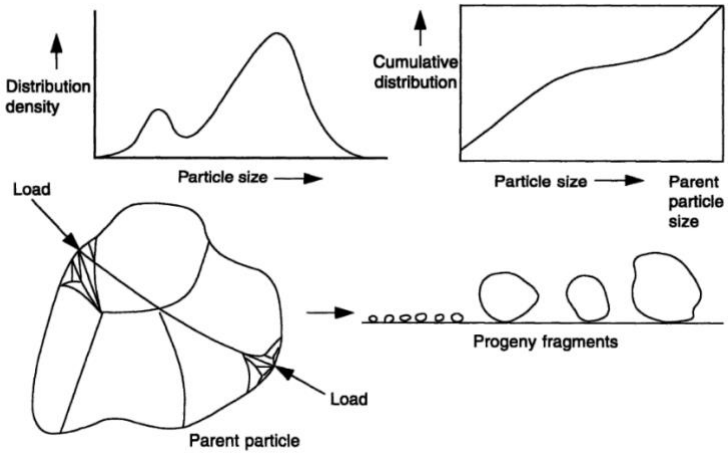

Figure 2-4 Cleavage fracture mechanism with particle size distribution (King, 2001)

The third pattern of fracture is said to be attrition and chipping. The attrition usually takes place when the size of the particle is large, but the stress present is not large enough to cause this breakage (Figure 2-5). The original particle is somewhat not broken and stays in the same shape and size, but some tiny particles are chipped from the original parent particle. This results in the product size distribution with two peaks separated by a range of sizes with no particles size in between.

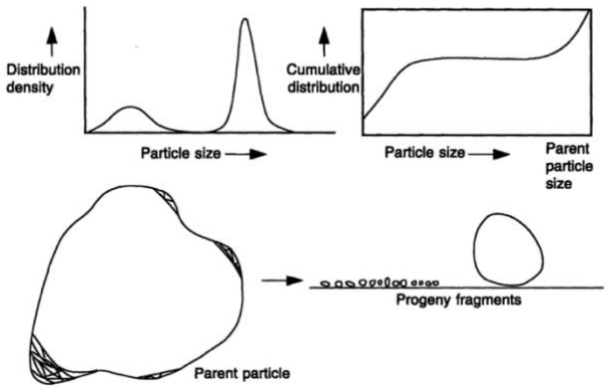

Figure 2-5 Attrition and chipping fracture mechanism with particle size distribution (King, 2001)

2.2.2 Comminution Energy

In the late 1950s, Bond presented few principles to explain the process of comminution (Bond, 1961) which became the point of reference to evaluate energy required to break certain material. Firstly, he mentioned that the difference between the feed and product energy levels should be equal to the energy given/input during crushing or grinding. Secondly, he presented the principle that the increase in the length of the cracks in the particle is proportional to the energy input. Thirdly, he explained that the weakest crack/flaw in the particle would govern the breaking strength of that particle. These laws then paved the way for accessing the energy required during the comminution of ores/rocks. Bond presented the work index (Wi) idea, which states that the energy required to reduce a ton of ore from infinite size to a size where 80% of material is passing 100 µm. The work index can be calculated at a laboratory scale using Equation 1.

$$W_i = \frac{44.5}{P_1^{0.22} G^{0.82} \left(\frac{10}{\sqrt{P}} - \frac{10}{\sqrt{F}}\right)} \quad (1)$$

Where Wi is the work index (kWh/st), P_1 is the required product size (µm), G is the grindability of the ore (g/revolution), P is the product 80% passing size (µm), and F is the feed 80% passing size.

This Work Index can then be used to calculate the energy required in the grinding stage of processing by using Equation 2.

$$W = W_i \sqrt{\frac{100}{P}} \left(1 - \frac{1}{\sqrt{\frac{F}{P}}}\right) \quad (2)$$

Where W is the required energy during the grinding stage (kWh/st).

2.2.3 Crushing Stages

Crushing of ore particles is a dry process carried out in a series of stages by either of two mechanisms: compression of the particles against any rigid surface or using impact force on the surface of particles constrained in a limited area.

The first stage is referred to as primary crushing, which employs a rugged jaw or gyratory crusher to reduce the ROM feed size to around 20 cm (S.K. Haldar, 2013). The secondary crusher is lighter than the primary machines and mainly employs the cone crusher. As a result, the product size after the secondary crushers is almost in the range of 0.5 – 2 cm. If, after secondary crushing, the ore size is still considerably large to be used in grinding operations, then tertiary recrushing is recommended, which uses the secondary crusher in a closed circuit. This crushing is required when the ore material is hard or if there is some requirement to minimize fines production.

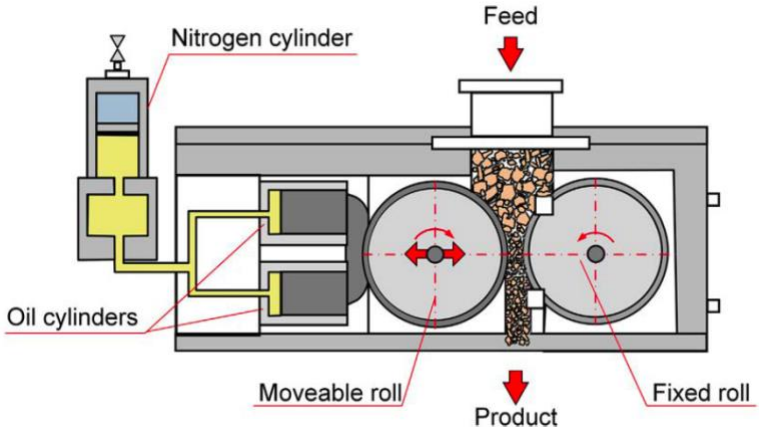

Figure 2-6 Schematic of high pressure grinding roller (Barry A. Wills et al., 2016b)

In the late 1980s, work by Prof. Schönert of Germany introduced the idea of a High-Compression Roller mill, a new type of crushing mechanism which was later coined as High Pressure Grinding Rolls (HPGR) (Schönert, 1988). This mechanism helped to increase the exerted pressure on feed significantly. The conventional methods used the pressure of around 10-30 MPa for crushing, which was increased to even 150 MPa by HPGR. These roll mills used the compression action on the bed of particles that were present between two rollers. Thus, feed crushing happened mainly due to the inter-particle crushing in the constraint environment between rollers. This mechanism

reduced the energy consumption significantly and also has less wear and reduction in over-grinding (Schönert, 1988). The schematic of HPGR can be seen in Figure 2-6.

2.3 Particle Size Distribution

In mineral processing, the particles of minerals never consist of one size. Instead, they have different shapes and sizes, making it difficult to estimate the size of the particle. Moreover, as the particles are not in any proper geometrical shape like spheres or cubes, the exact measurement of the size of the particle is not possible.

There are different ways to estimate the size of such an irregular particle, but none of the methods can predict the exact measurement. For example, one method is to determine the size of the particle by letting it pass from a hole or aperture. Another method used to measure the circle's diameter possesses the same cross-sectional area as the particle itself. The other few methods to measure particle sizes are optical methods or electron microscopes, which can even go to 0.001 µm measurement (Gupta & Yan, 2016). The size data should also be accompanied by the remarks for the shape of the particle.

2.3.1 Particle Size Analysis

Particle size analysis of the products is used to determine the optimum size of the feed to reach maximum efficiency (Barry A. Wills et al., 2016a). This analysis is also essential to determine the size range at which any losses occur in the plant to reduce them. Different methods are in practice for particle size estimation. Some of these methods are enumerated in Table 2-1.

One of the oldest and most widely used methods of particle size analysis is test sieving. It is very widely used in industry, and with current practices, the particles sizing can be done down to about 5 µm. The known weight passes through successive finer sieves and then weighs the collected material's sample weight on each. This sample weight on each sieve is then converted to the percentage weight of each size fraction. There are few factors that need to be kept in mind while undergoing the process of test sieving. First, the time given for sieving of the sample should be enough so that all particles on the top sieve should get a chance to meet the sieve aperture. If the particles are small, they will pass the aperture, and if they are more in size to pass through the

sieve, they will remain on the sieve. Secondly, the test depends on the amount of material put in the sieve, also known as 'charge.' If the charge of sample material will be large, it will not allow all the particles to reach the aperture pass through it. Few techniques are used to avoid such obstacles. One such way is to use 'air-jet sieving' in which air is blown onto the sample, which decreases the testing time and allows particles to move and reach the apertures of the sieve.

Table 2-1: Different methods of particle size analysis (Barry A. Wills et al., 2016a)

Method	**Wet/Dry**	**Fractioned Sample?**	**Approx. Useful Size Range (µm)**
Test sieving	Both	Yes	5 – 100,000
Laser diffraction	Both	No	0.1 – 2,500
Optical microscopy	Dry	No	0.2 – 50
Electron microscopy	Dry	No	0.005 – 100
Elutriation	Wet	Yes	5 – 45
Sedimentation (gravity)	Wet	Yes	1 – 40
Sedimentation (centrifuge)	Wet	Yes	0.05 – 5

The data obtained from any size analysis methods are used to understand the size distribution of the particles in mineral processing. The mean size of particles retained and passing on the sieves somewhat explains the particle size within the sieve ranges. The percentage passing or percentage retained on sieves are tabulated and graphed, but it seldom follows a linear relation, making it hard to get the particle size data other than the sieve size used. This led to the formulation of some models that can estimate the particle size from the particle size distribution.

2.3.2 Particle Size Distribution Models

As explained above, the size distribution of particle samples hardly obeys linear relationships and seldom forms a normal distribution pattern. The particle size distribution is mainly skewed to the right of a graph. In addition to skewness, many-particle size curves are S-shaped, with most of the data congested towards the two ends of the graph. In order to avoid such skewed data and get better estimation and knowledge of particle size, few models were formulated by different researchers, which are discussed in the following paragraphs (Gupta & Yan, 2016).

2.3.2.1 Log-Normal Distribution

Log-normal distribution helps shape a skewed data graph into normal distribution by using the log scale for the x-axis and probability scale as the y-axis of the graph. The x-axis has sieve/aperture size against y-axis representing cumulative percentage passing. Although the probability scale is inverse normal distribution, if you plot a normal distribution, it can give a simple straight line that can be used to estimate the other values of the data by interpolation. Moreover, the normal distribution can be used to measure the mean of distribution which will be equal to 50% passing size or d_{50}.

2.3.2.2 Gates-Gaudin-Schuhmann (GGS) Distribution

Gates-Gaudin-Schuhmann (GGS) distribution method is one of the most widely used methods for relatively coarser particle size data (Gupta & Yan, 2016). This method uses equations to represent particle size distribution curves and is used for non-uniform size distribution.

In the GGS method (Schuhmann, Jr., 1940), both x and y axes are of a log-log scale, and the graph is plotted between cumulative passing data and the sieve size. This will normally give the linear plot from which data can be interpolated easily. The advantage of this plot is that it can provide the size of particles by using even a small number of sieves. This plot expands the region of the plot below 50% but shrinks the region of the plot above 50%, passing, which is a slight disadvantage of this method. This linear trend fits in the following equation.

$$\log \mathrm{P} = \alpha \log \frac{\mathrm{X}}{\mathrm{K}} + \log 100 \tag{3}$$

This can be simplified as follows

$$\mathrm{P} = \log\left(\frac{\mathrm{X}}{\mathrm{K}}\right)^{\alpha} \tag{4}$$

Where P is the cumulative passing data (%), X is the particle size, K is the size parameter, and α is known as the distribution coefficient (Austin et al., 1984). The slope of the straight line of the plot will give the distribution parameter α. The intercept of the straight line when P = 100% will give the size parameter K. The size parameter K measures the top size, whereas the distribution parameter talks about the narrowness and broadness of the particle size distribution.

2.3.2.3 Rosin-Rammler (RR) Distribution

Rosin-Rammler (RR) distribution method is also among the most widely used methods, especially relatively finer particle size data (Gupta & Yan, 2016). This method also uses an equation to represent particle size distribution. It is mainly used to represent the results of the data of particles obtained by grounding in ball mills or tumbling mills. This method is used in the mineral processing of coal, for which it was developed in the first place.

In the RR method (Rosin & Rammler, 1933), the graph is plotted between the log of sieve size on the x-axis and double log of cumulative retained data on the y-axis, i.e., log (log 100/R) where R is the retained mass in percentage. This plot expands the region at the finer and coarser ends (< 25% and >75%) but shrinks the region between, i.e., 30 – 60 % of the plot. The RR distribution is expressed as

$$\log \left[\ln \frac{100}{100\text{-R}}\right] = \log \text{b} + \text{n} \log \text{X} \tag{5}$$

The above can be simplified as follows

$$100\text{-R} = 100 \exp(\text{bX})^{\text{n}} \tag{6}$$

Where R is the cumulative retained data (%), X is the particle size, b is the size parameter, and n is known as the distribution coefficient (Austin et al., 1984). The slope of the straight line of the plot will give the distribution parameter n. The intercept of the straight line when P = 100% will give the size parameter b. The size parameter b measures the top size, whereas the distribution parameter talks about the narrowness and broadness of the particle size distribution.

2.4 Microwave (MW) Irradiations: Heating Principles and Impact on Processing

The high energy demand during the comminution of ores stemmed from the process of preheating ores before comminution. This process is done by repeated heating and cooling of rocks to induce intergranular cracks. These cracks are generated due to the expansion and contraction of the granular structure (Fitzgibbon & Veasey, 1990). It was reported that these cracks result in better liberation of minerals, reducing the fines in the downstream process, better grinding, and less plant wear and tear (King & Schneider, 1998). This process is termed Thermally assisted liberation

(TAL). However, although liberation achieved by preheating was advantageous in few terms, it was still not efficient in terms of energy (Fitzgibbon & Veasey, 1990).

Inefficiency in terms of energy in normal heating processes paved the way for more new pre-heating the ores. As in conventional heating techniques, the complete ore is getting heated, which is not that efficient. Therefore, targeted heating of some minerals was the main aim of treating the samples with microwave irradiation. Güngör and Atalay in 1998 reported that the generation of cracks inside the mineral grain could be achieved when it is composed of minerals that have different heating properties when exposed to microwaves (Güngör & Atalay, 1998).

The use of microwave energy has increased manifold after their discovery during World War II. Now, these are in use almost in every sphere of life. May it be telecommunication, medical or domestic use, it is used in one or the other. In recent past two decades, one of the applications of microwave energy has been seen in mineral processing, particularly in comminution, which is undergoing many developments and has been found beneficial.

2.4.1 Microwaves: Definition and Maxwells Equations

Microwaves are part of the electromagnetic spectrum with frequency ranging from 300 MHz to 300 GHz, but the most common frequency on which microwaves work is 2.45 GHz (Haque, 1999), and wavelength of microwaves range between 0.1mm to 100 cm. The speed of microwaves in free space is the same as that of light, i.e., approximately 3×10^8 m/s. The composition of the microwave machine itself can be divided into four components: applicator (oven), a power supply, a magnetron and a waveguide which provides a pathway for microwaves from the generator to reach the applicator (Smith, 1984), as shown in Figure 2-7. The microwaves can be advantageous due to short start-up time, precise control of the specification during the process and volumetric heating of the materials. So are other advantages of microwave heating over conventional heating techniques (Haque, 1999).

1. No contact is required for heating.
2. The heating takes place due to energy transfer and not due to heat transfer.
3. Rapid, material selective and volumetric heating takes place.
4. The heating process through microwaves starts from inside of the material body.

5. There is a high level of safety and automation.

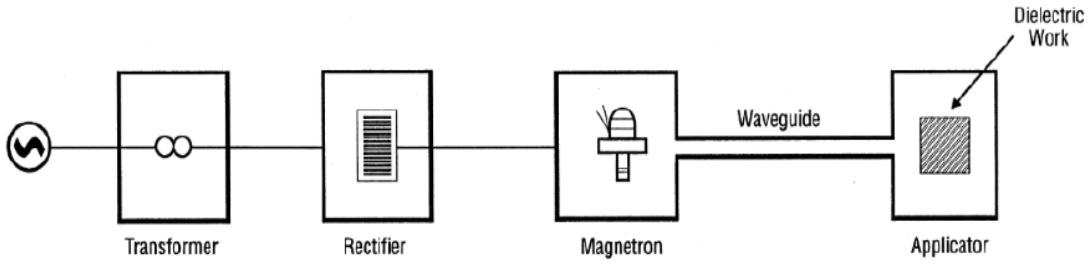

Figure 2-7 Simplified schematic of microwave system (Smith, 1984)

Microwaves consist of electric and magnetic fields which transmit in the form of a wave. The interaction between the two fields, i.e., electric and magnetic and with the source takes place by the following Maxwell equations (Griffiths & Inglefield, 2005):

$$\nabla \times E = -\frac{\delta B}{\delta t} \tag{7}$$

$$\nabla \times B = \mu_o \varepsilon_o \left(\frac{\delta E}{\delta t}\right) + \mu_o J \tag{8}$$

$$\nabla \cdot E = \left(\frac{1}{\varepsilon_o}\right) \rho_c \tag{9}$$

$$\nabla \cdot B = 0 \tag{10}$$

Where E is the electric field, B is the magnetic field, μ_o is the permeability of free space, $\varepsilon_o$is the permittivity of free space, ρ_c is the charge density, J is the current per unit area perpendicular to flow. The Equations 7-10 describe the electromagnetic waves passing through the free space. However, when some materials, like conductors and insulators, are present, these equations change and take a new shape. For example, in the case of conductors, the charge density ρ_c flows almost instantaneously to the surface, whereas in the case of insulators, the charge density ρ_c has no value as there is no free charge available due to tightly bonded atoms.

2.4.2 Microwave Heating Mechanism

The materials are classified into three different categories based on their response to the exposure of microwaves: (i) Transparent/insulators like ceramics which do not absorb any microwaves and

let them pass without any effect; (ii) Conductors like aluminum which reflect microwaves and do not let them pass through; (iii) Absorbers like basalt which partially absorbs the energy-producing heat and transmit the rest (Pozar, 2005)(Haque, 1999). These materials can be seen in Figure 2-8.

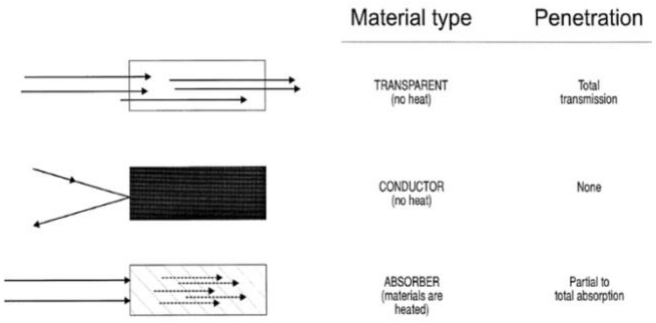

Figure 2-8 Types of material based on their response to EM waves (Haque, 1999)

Absorbers like basalt react differently to microwaves due to their permittivity and permeability. Both these properties are complex numbers and are a combination of two factors: (i) Dielectric constant, which is the ability of the material to delay the microwaves to pass through them (Haque, 1999) or, in other words, the ability of the material to store charge, and (ii) the loss factor which ascertain the loss of energy in the material due to dissipative process (Collin, 2010) or it can be told that the loss factor is the ability of the material to release the stored energy in the form heat (Al-Harahsheh et al., 2009). These factors were considered by (Saxena, 2009) to model the complex behaviour of electric and magnetic waves in matter. The equations are:

$$\varepsilon^* = \varepsilon' + i\varepsilon'' \quad (12)$$

$$\mu^* = \mu' + i\mu'' \quad (13)$$

Where ε' (dielectric permittivity constant) and μ' (dielectric permeability constant) are considered the real parts of the equations responsible for the normal dynamics of the material. ε'' (permittivity loss factor) and μ''(permeability loss factor) are considered the complex imaginary parts representing the losses taking place in the material due to the response shown towards electric and magnetic fields, respectively. The rock materials mostly respond to electromagnetic waves due to electric field intensity and not because of magnetic field intensity, as most rock materials are non-magnetic.

2.4.2.1 Electrical Conductivity of Materials

Equation 14 (Gabriel et al., 1998) describes the relationship between material electrical conductivity and loss factor.

$$\sigma = 2\pi f \varepsilon_o \varepsilon'' \quad (14)$$

Where σ is the electrical conductivity of the material, $2\pi f$ is the angular frequency in Hz, ε_o is the free space electrical permittivity (8.86×10^{-12} F/m) and ε'' is the material loss factor at the given frequency.

2.4.2.2 Loss Tangent

The loss tangent is also a parameter used to determine the amount of energy that is lost within a material and is given by Equation 15.

$$\tan\delta = \frac{\varepsilon''}{\varepsilon'} \quad (15)$$

where $\tan\delta$ is the loss tangent, ε'' is the loss factor and ε' is the dielectric constant. This relationship suggests that more loss tangent will result in more loss factors. Also, considering Equation 15, the bigger the loss tangent, the bigger is electrical conductivity which means more energy absorption by the material.

2.4.2.3 Power Density

Electromagnetic waves are helpful because they transport energy while passing through space. The power density generated by the electrical field of a unit volume absorbed by a non-magnetic material when it is exposed to electromagnetic field is measured by Equation 16 (Al-Harahsheh et al., 2009):

$$P = 2\pi f \varepsilon_o \varepsilon'' E^2 \quad (16)$$

Where P is the power density (W), and E is the electrical field strength inside the material (V/m). The first law of thermodynamics explains that the power absorbed or released within a mass of material increases the temperature of that material and is given by Equation 17 (Meredith, 1998):

$$P = mC_p\left(\frac{\Delta T}{\Delta t}\right) \quad (17)$$

Where P is the power absorbed (W), m is the mass of material (kg), C_p is the specific heat capacity of material (J/kg^{o}C), ΔT is the temperature difference during the time interval of Δt.

2.4.3 Effect of MW Heating on Minerals

The microwaves transport energy into the material, leading to temperature increases due to the heat generated inside the material. The rocks are composed of several different minerals. Some of these minerals are good absorbers, whereas some are transparent to microwave exposure. This is due to the different dielectric values of minerals. Minerals with different dielectric properties combine to form rocks with entirely new dielectric properties (Motlagh, 2009). The first research on the treatment of minerals by microwaves was studied in 1967 by Ford and Pei. Microwaves heated the metal oxides and sulphides, and a subjective relation was established between heating rates and the colour of the mineral. It was recorded that the minerals with darker colours showed more excellent heating rates than lighter-coloured minerals.

In 1984, Chen et al. carried out a study to measure the temperature of 40 pure minerals when they were exposed to microwave irradiation for 3-5 min at 150 W power and frequency of around 2.45 GHz (Chen et al., 1984). He concluded that sulphides and metal oxides were microwaves absorbers, whereas silicates, carbonates and some oxides showed a transparent response to the microwave irradiations. Similar work was carried out by Walkiewicz, who confirmed the findings of Chen et al. (J. W. Walkiewicz et al., 1988).

Moreover, in 1988, Church et al. (1988) also researched the effect of microwaves on minerals. He categorized six mineral classes: oxides, carbonates, silicates, phosphates and sulphates, haloids and tungstates as weak microwaves absorbers and called them ‘low loss minerals’ (Church et al., 1988). These minerals were treated in powdered form at frequencies range of 0.3 to 1 GHz.

A new technique to quantify the inductive heating within a microwave cavity on subsequent rock fragmentation was proposed by Hassani (Hassani et al., 2020). They used a novel calorimetric technique to get the idea of induced heat on the samples and presented a new parameter that can evaluate the effects of microwave-induced energy and thermally induced fracturing. The cylindrical samples of basalt and kimberlite were treated in microwaves at 10-15 kW power levels for 10 – 40 seconds. These samples were then immediately put in the calorimeter for energy analysis. The standard calorimeter method was used to determine how microwave energy is converted into heat in a material (Adl-Zarrabi, 2006). Equations 18 and 19 were used to calculate the sample temperature after treating it with the microwave.

$$m_r C_{p,r}(T_r - T_{eq}) = m_w C_{p,w}(T_{eq} - T_w) \quad (18)$$

$$T_r = T_{eq} + \frac{m_w C_{p,w}(T_{eq} - T_w)}{m_r C_{p,r}} \quad (19)$$

Where T_{eq} is the temperature obtained from the calorimeter, m_r is the mass of the sample, m_w is the mass of water, $C_{p,r}$ is the specific heat capacity of the rock sample, $C_{p,w}$ is the specific heat capacity of water, T_r is the final temperature of the rock sample, and T_w is the initial temperature of water.

This study proposed a new parameter for energy analysis that describes the efficiency of converting microwave energy into sensible heat within the rock. This parameter was named Heat over Microwave Efficiency (HOME), which is the ratio of heat absorbed to the microwave energy input and is given by Equation 20:

$$\text{HOME} = \frac{\text{Heat Absorbed}}{\text{Total Microwave Energy}} = \frac{m_r C_{p,r}(T_{i,r} - T_r)}{P_{in}\Delta t} \quad (20)$$

Where $T_{i,r}$ is the initial temperature of the sample, P_{in} is the microwave power input, and Δt is the microwave exposure time.

Similarly, another parameter was introduced in the same study to represent the strength reduction by microwaves eliminating the dependency on UCS measure of material strength. The parameter was named "Weakening over Microwave Energy" (WOME). It is defined as the percentage reduction achieved per microwave energy input measured in units of kWh/t.

2.4.4 Impact of MW on Rock Strength and Comminution

The use of microwave irradiations on increasing mineral liberation and reducing energy consumption during comminution has been in studies for the last few decades. The microwave's exposure to rocks transports energy which is either absorbed, transmitted or reflected by the rocks depending on the properties of minerals. Due to this difference in mineral properties, some

minerals/grains get heated due to microwave energy. This mechanism creates thermal stress and gradients inside the rock as the minerals possess different thermal expansion coefficients. The thermal stresses result in intergranular cracks rather than intragranular cracks (Kingman & Rowson, 1998). This increases the energy efficiency during comminution and avoids over-grinding, reducing fine production (Guo et al., 2011) (Wang & Forssberg, 2005). Although, this process is beneficial in energy reduction during comminution, the improvement is still insufficient to compensate for the energy given during microwaving.

In 1990, Fitzgibbon introduced the concept of microwave-assisted comminution, mainly grinding (Fitzgibbon & Veasey, 1990). Mainly, the effects of microwaves on rock strength were measured by use of different tests like the Uniaxial Compressive Strength (UCS) test, Brazilian Tensile Strength (BTS) test and Point Load Strength (PLS) Test. In 2000, Kingman carried out several studies on the effect of microwave irradiation on mineral processing, including grinding, leaching, and mineral separation. He evaluated the grindability of ilmenite, sulphide, high refractory gold and carbonite ore by analyzing the Bond Work Index (BWI). The samples were exposed to variable power microwaves of up to 2.6 kW at different exposure times. The study concluded that microwaves could significantly reduce the BWI of ores which can be beneficial in reducing energy consumption during comminution microwave (Kingman et al., 2000). Vorster studied the impact of microwaves on copper ore and reported that a 70% reduction in work index could be achieved after exposing the samples for 90 s to a 2.6 kW power microwave in the multi-mode cavity (Vorster, 2001). Moreover, increasing the power level of microwaves also decreases the BWI of the ores (Sahyoun et al., 2004).

The effect of short-term microwave exposure, at high power levels and also with pulsed delivery of radiation found to be an effective method too. Kingman researched 1 kg copper carbonite ores with power levels ranging from 3 kW to 15 kW in a single-mode cavity. The author concluded that a 30% reduction in impact breakage parameter was achieved with exposure of just 0.2 s at 15kW of power (Kingman, 2006). Wang and Forssberg presented microwave-assisted comminution on different minerals like dolomite, limestone, copper ore, and quartz (Wang & Forssberg, 2005). The used microwaves with a power of 3 kW and 7 kW with exposure time up to 30 minutes. The UCS tests and dry ball milling tests were carried out to compare the effects of microwaves on treated and untreated samples. The UCS strength of quartz and limestone was reported to be reduced from

50 MPa to 25 MPa and 40 MPa to 35 MPa. He also suggested from the results of grindability tests that the microcracks generation favoured the energy reduction in the comminution processes.

The effect of microwave irradiation on kimberlite ore has also been studied in the recent past. Kobusheshe conducted some experiments on the effect of microwaves on two types of kimberlites which contain a substantial amount of hydrated minerals (Kobusheshe, 2010). The author reported a 40% reduction in point load strength of the kimberlite ore test sample when treated at 17s at 12kW power with input energy of around 9kWh/t.

One of the recent studies in kimberlite recorded a significant decrease in the UCS strength of kimberlite. Cylindrical rock samples were treated at different power levels (2 – 15 kW) and exposure time. It was concluded in the study that at 15 kW microwave power and exposure time of around 40 s, the cylindrical rock sample disintegrated showing the strength reduction in the kimberlite rock samples (Deyab et al., 2021). The results for HK kimberlite sample at different power levels are shown in the Figure 2-9.

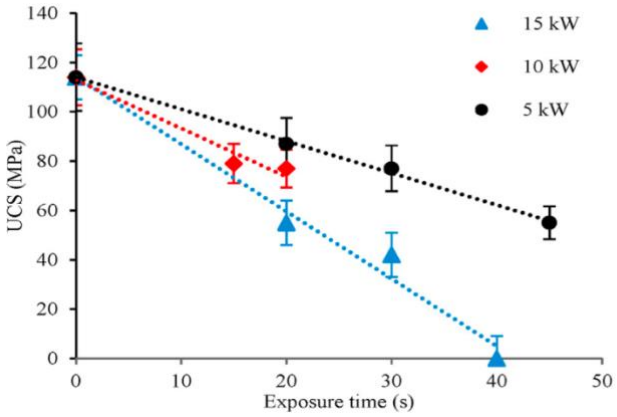

Figure 2-9 Unconfined compressive strength reduction for kimberlite sample (Deyab et al., 2021)

2.4.5 Impact of MW on Particle size

All materials respond differently to microwaves exposure due to different dielectric properties. The size of particles is also an essential parameter while considering the impact of microwave irradiations. One of the studies on metal oxides carried out by Walkiewics in 1988 concluded powdered metal oxides showed a better response towards getting heating than their bulk

counterparts (J. W. Walkiewicz et al., 1988). The study by Wang and Forssberg showed that microwaves exposure has a significant effect on the particle size of limestone, quartz dolomite inducing better liberation and improved fineness of the ground product (Wang & Forssberg, 2005). Crane stated that the particle size of iron oxides, which is non-conductive, showed an inverse relationship with microwave absorption. He reported that decreasing the size of particles increased microwave absorption. Whereas in the case of conductive metals like aluminum and copper, decreasing the particle size resulted in decreased microwave absorption (Crane et al., 2014).

3. Methodology and Experimental Setup

This chapter introduces and presents the methods employed for studying the effect of Microwaves-assisted crushing of kimberlite ore by considering the size and energy as the analyzing criteria.

3.1 Materials

3.1.1 Mineralogy of Rock Samples

Kimberlite, an igneous rock, is the primary source of diamonds. The rock type for this study was Hypabyssal Kimberlite (HK) obtained from Gahcho Kue Mine of DeBeers, in Northwest Territories of Canada. The rock samples were obtained in the form of drill cores (Figure 3-1). Few of these rock samples were selected, crushed and pulverized to get to know the mineralogy of these samples by using the X-ray diffraction (XRD) technique. The results obtained by the XRD are as shown in Table 3-1. These results show that HK kimberlite samples are mainly composed of mica and a serpentine group of minerals which fall under the category of silicates. The composition of HK kimberlite also has carbonates around 19.4% and oxides around 9.1%. Among all these minerals, magnetite has the maximum potential of absorbing microwave irradiations, whereas the silicates and carbonates have meagre potential to be heated by microwave irradiations.

Figure 3-1 Drill core samples of kimberlite

Table 3-1: Mineral composition of HK kimberlite samples obtained from XRD analysis

Mineral	**Mineral Group (Class)**	**Composition (%)**
Clinochrysotile	Serpentine (Silicates)	34.1
Illite (phlogopite)	Mica (Silicates)	19.4
Calcite	Calcite (Carbonates)	18.4
Magnetite	Spinel (Oxides)	9.1
Vermiculite	Mica (Silicates)	6.4
Microcline	K feldspar (Silicates)	5.9
Clinochlore	Chlorite (Silicates)	4.5
Albite	Plagioclase (Silicates)	2.2

3.1.2 Properties of Rock Samples

Different properties of HK kimberlite rock samples were measured to get to know the homogeneity of all samples. The properties and the method employed to measure those properties are explained below.

3.1.2.1 Specific Gravity

Specific gravity is an important physical property of rocks and minerals. The specific gravity of samples can give the idea of the homogeneity of different samples of the same rock. The specific gravity of HK kimberlite was measured using the water displacement method. Fourteen samples were used to measure the specific gravity of rock samples which came out to be 2.56 g/cc with a standard deviation of ± 0.013 g/cc.

3.1.2.2 Moisture Content

The moisture content of the rock samples was measured to determine the presence of moisture inside the rock samples of HK kimberlite. The presence of water inside the samples can affect the heating of rock by microwaves. The moisture content was determined by measuring the reduction

in mass of the sample after the standard heating procedure. From measurement on seven samples, the average moisture content was found to be 2.4%, with a standard deviation of around ± 0.11%.

3.1.2.3 Dielectric Property

The response of the material to microwaves is characterized by its dielectric properties. The dielectric properties of materials can be measured by the coaxial probing method. The dielectric properties of HK kimberlite were taken from the previous work on kimberlite (Deyab et al., 2021). The permittivity values ranged between 7.7 at 2.45 GHz and 6.4 at 12 GHz (Figure 3-2). The imaginary permittivity value was 1.07 at 6.94 GHz, and the loss tangent was highest at 0.15 at 7.5 GHz (Figure 3-3).

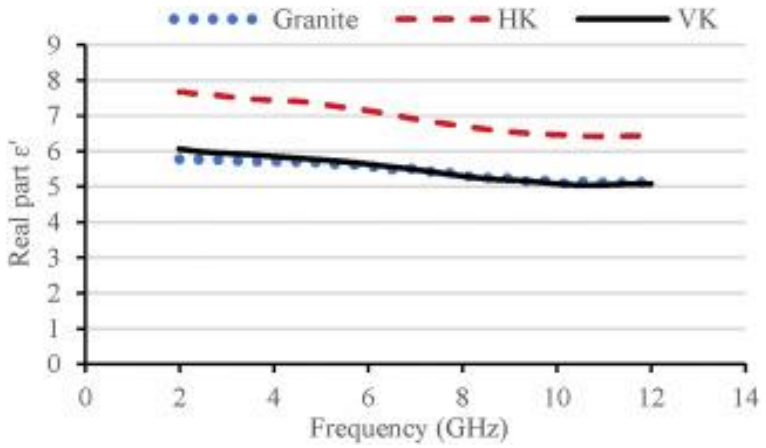

Figure 3-3 Real part of complex permittivity for HK samples (Deyab et al., 2021)

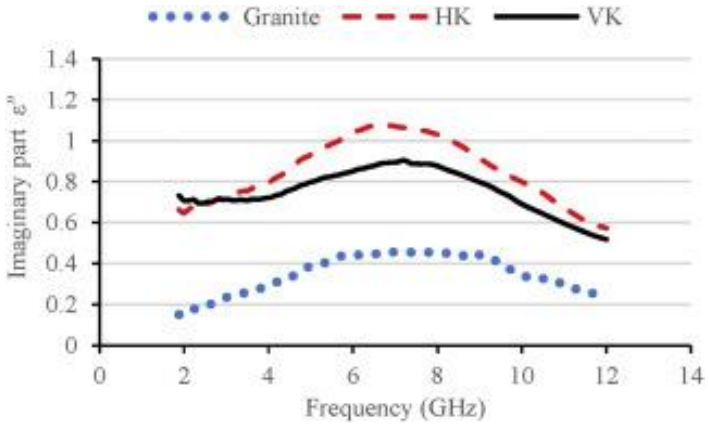

Figure 3-2 Imaginary part of complex permittivity for HK samples (Deyab et al., 2021)

3.2 Equipment

3.2.1 MW System

The HK kimberlite samples were treated using a 5-15kW power output capacity microwave available at the Geomechanics laboratory of McGill University, as shown in Figure 3-4. The microwave consists of a magnetron capable of generating 2.45 GHz electromagnetic wave frequency which is almost equal to 12.2 cm wavelength. The control panel was used to adjust the power and exposure time as per the design of the experiments. Through a pyramidal horn antenna, the magnetron-generated waves passed through the WR340 waveguide into a 60 x 60 x 60 cm metallic box cavity. This antenna located at the end of the waveguide prevented the incoming electromagnetic waves from scattering randomly in all directions. The microwave was capable of working both in the single and multi-mode system. Microwaves are primarily used in the multi-mode system as it chaotically transmits the electromagnetic energy inside the cavity. On the other hand, a single-mode microwave focuses the microwave energy to a certain area by constructing positive interference between incident and reflective waves. Previous microwaves suggested that single-mode microwaves worked better as they could translate higher power density in concentrated areas (Hassani et al., 2020). For this reason, the study was conducted in the single-mode microwave.

Figure 3-4 Industrial microwave system with variable high power (up to 15 kW) in Geomechanics Laboratory at McGill University

3.2.2 Crushing System

The crushing of HK kimberlite samples was carried out by using a laboratory scale single roll crusher. The single roll crusher used the compressive force as the breakage mechanism. The breakage mechanism used in single roll crusher is somewhat similar to industrial high pressure grinding rolls (HPGR). The crusher model used for our microwave assisted crushing study was SQ110VEL manufactured by Goldbelt Global. The crusher system can be seen in the Figure 3-5. The single-roll crusher consists of a feed hopper (1) and the crushing chamber (2) electrically powered by a 746 Watts motor using a 110-volt AC circuit. The motor runs the drive chain, which connects to the main roller shaft and rotates the roller. The feed throat size was 76.2 x 92.25 mm. The discharge size was set at a maximum of 6 mm. A bucket (4) was installed at the crusher discharge to collect all crushed material. A digital data logger (3) was attached to the crusher system, which gave them power and energy consumption values while crushing the samples.

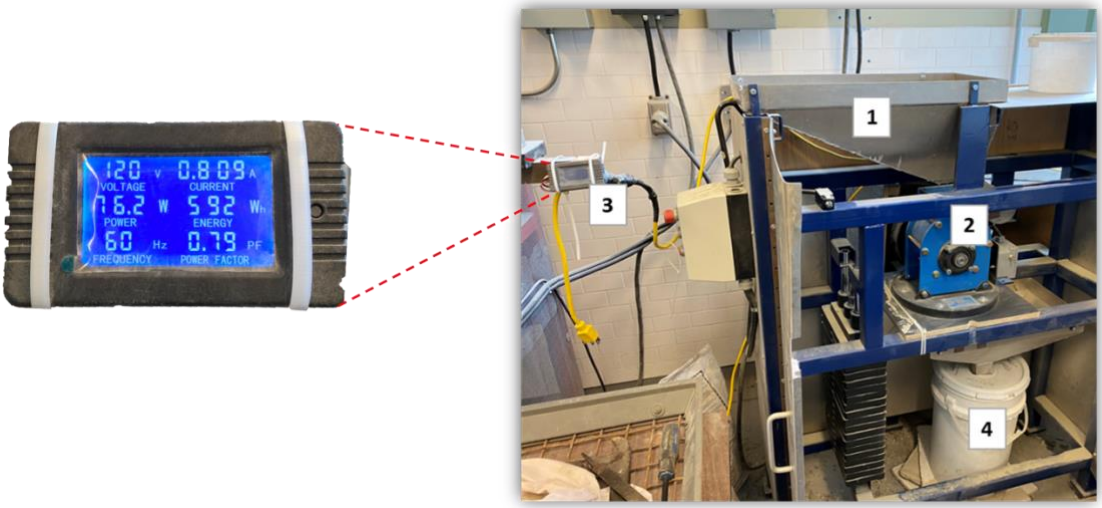

Figure 3-5 Single roll crushing setup at Geomechanics Laboratory at McGill University

3.3 Methodology

3.3.1 Sample Preparation

The HK kimberlite rock samples from Gahcho Kue Mine were attained in the form of drill cores. Approximately 100 kilograms of these drill core samples were sieved at 50 mm, and the oversize

fraction was then pre-crushed by a laboratory jaw crusher available at the Mineral Processing Laboratory of McGill University. The crushed material and the undersize samples, obtained from cores, were then mixed and classified by Gilson screen shaker and ROTAP shaker at seven sieve sizes: 31.5, 26.5, 19, 16, 12.7, 9.5 and 6.7 mm with d_{50} of around 16 mm. Later, these samples were divided into two classes (SC): SC_1 ranged between 31.5 – 16 mm, and SC_2 ranged between 16 – 6.7 mm. The samples of 500 g of each size class were then made to be treated in the microwave under different microwave conditions (Figure 3-6). However, this thesis's research work is limited to the impact of MW on SC_1 samples of HK.

Figure 3-6 500g of particulate HK sample

3.3.2 Density and Moisture Content Measurement

The density of the rock samples was measured using the water displacement method. The mass of the samples was measured using an electronic scale. A container was filled with water and placed on an electronic scale. The samples were put in a nylon bag whose weight was measured before putting the samples. The rock samples in the nylon bag were then hanged above the water container with the help of a tripod stand. The hanging rock samples were then lowered and submerged in the water. The change in the weight of the water due to submerged rock samples was noted, which was the volume of the rock samples. As the density of water is 1 g/cc, the specific gravity of rock samples was found using the equation below.

$$\text{Density}\left(\frac{\text{g}}{\text{cc}}\right) = \frac{\text{Mass of dry samples}}{\text{Volume of sample}} = \frac{\text{Mass of dry sample}}{\text{Mass of water displaced} - \text{Mass of nylon bag}} \quad (21)$$

$$\text{Specific Gravity} = \frac{\text{Density of rock samples}}{\text{Density of water}} \quad (22)$$

The moisture content of HK kimberlite samples was measured by determining the reduction in mass of the sample. Few of the representative samples were selected, and their initial mass was recorded using the electronic balance. These samples were then placed in a lab oven at a temperature of around 110 ± 5 °C. The weight of samples was measured again after 24 hours when they dried entirely in the oven. The average moisture content was found to be around 2.40%.

3.3.3 Experimental Design

The two variable parameters were chosen to be studied in this research work: Microwave power and energy. Apart from these variables, some parameters were kept constant after preliminary tests observations, including the distance of the sample from the horn and mass of samples. The description of parameters is as below:

3.3.3.1 Microwave Power

As mentioned before, a 15-kW power microwave was used for this research study. To study the effect of microwave power on HK kimberlite samples, three power levels were chosen: 5, 10 and 15 kW, which represented the low, moderate and high power, respectively.

3.3.3.2 Microwave Energy Input

The second variable parameter chosen for the study was microwave input energy. The wide range of energy was between 5 – 270 kJ. The input energy was based on the exposure time of microwaves onto the sample. The energy was calculated using Equation 23.

$$\text{Input Energy (kJ)} = \text{Power(kW)} * \text{Exposure time (s)} \quad (23)$$

3.3.3.3 Particle Size

The HK kimberlite was divided into two size classes (SC), i.e., SC_1 and SC_2. The SC_1 ranged from 31.5 – 16 mm, and SC_2 ranged from 16 – 6.7 mm. The SC_1 was a relatively coarser size fraction as compared to SC_2. This was done in order to understand the effect of microwaves on coarse and fine-sized particles. However, the research work covered in the thesis was limited to only SC_1.

3.3.3.4 Constant Parameters: Mass of Sample and Distance from Horn

The mass of the HK kimberlite sample was kept constant for this study at 500 g. However, several preliminary tests were conducted to finalize the distance between the horn and sample particles. The tests were conducted at 18, 12 and 6 cm distance from the horn, and it was found that the optimum distance for these tests was 6 cm. However, the tests with a distance lower than 6 cm showed some sparks inside the microwave cavity, which is why the lower distance was neglected.

3.3.4 Testing Procedure

As mentioned above, 500 g particulate samples were prepared for MW treatment. Therefore, few samples were used to ascertain the properties of HK kimberlite samples. After determining the properties of the samples, the samples were then treated by microwaves.

The procedure adopted for the treatment of MW on samples is as shown in Figure 3-7. Each 500 g sample was placed on the flat non-microwave absorbing crucible. The surface temperature of the sample before microwave treatment was measured by taking the pictures using a Fluke TIS65-30Hz IR camera (Figure 3-8(a)). This camera captures the thermal image with IR-Fusion technology and has a resolution of 260 x 195 pixels. The image gave the surface temperature during the post-processing of thermal images using FLIR software provided by FLUKE Connect^{TM}.

After taking the image, the sample on a flat crucible was placed at a distance of 6 cm from the horn antenna inside the cavity using a non-microwave absorbing structure, as shown in Figure 3-8(b). The sample was then exposed to microwave irradiations. After microwave treatment, the sample was taken out. The picture was taken using a thermal camera to get the surface temperature of the sample after microwave treatment. The sample was then put in the calorimetric system

(Figure 3-8(c)), containing 1000 ml of water with initial measured temperature. After the temperature of water and samples reached an equilibrium, the final temperature was measured. Finally, the samples were taken out to be put in the oven for drying. The calculations for temperature change and HOME % are shown in Appendix B. However, the work for HOME % was carried out to check the samples' microwave efficiency and heat absorption and was not directly related to the focus of this research work, which was to analyze the effect of MW on product size and energy consumption crushing.

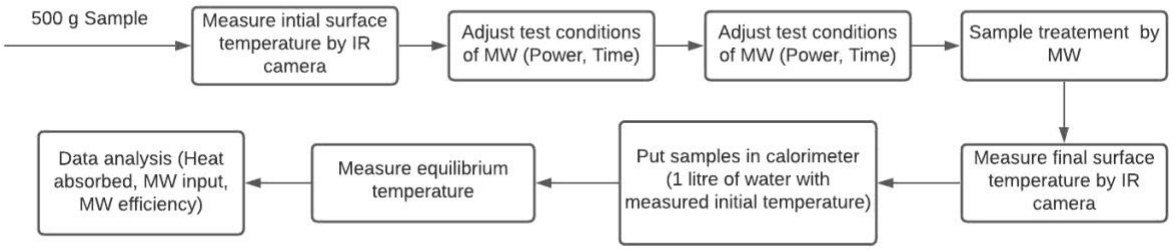

Figure 3-7 Experimental procedure for MW treatment of samples

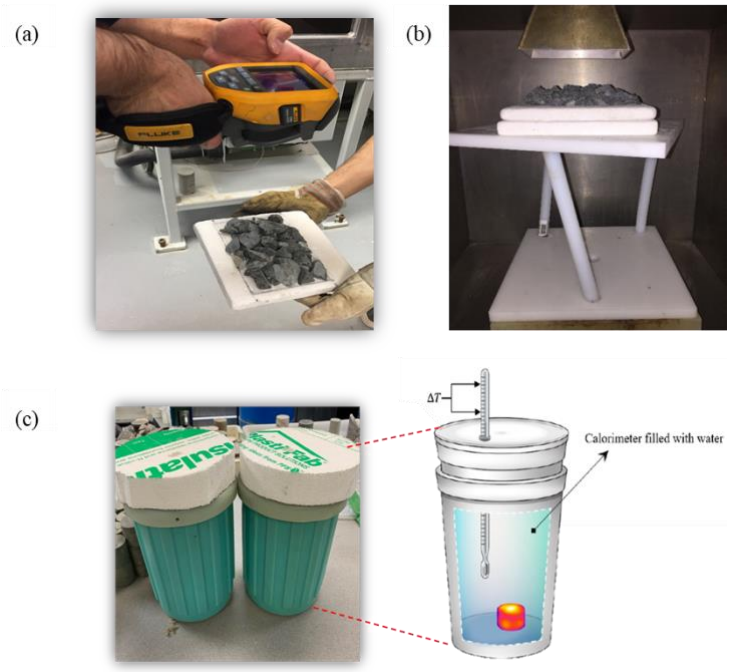

Figure 3-8 Microwave treatment of samples: (a) Thermal imaging by IR camera; (b) sample placement setup inside MW cavity; (c) calorimetric setup

After drying, the sample was placed in open air to reach the ambient temperature. After reaching at the ambient temperature, the sample was then put in the single roll crusher for crushing. The procedure followed during crushing and sieving of samples is shown in Figure 3-9.

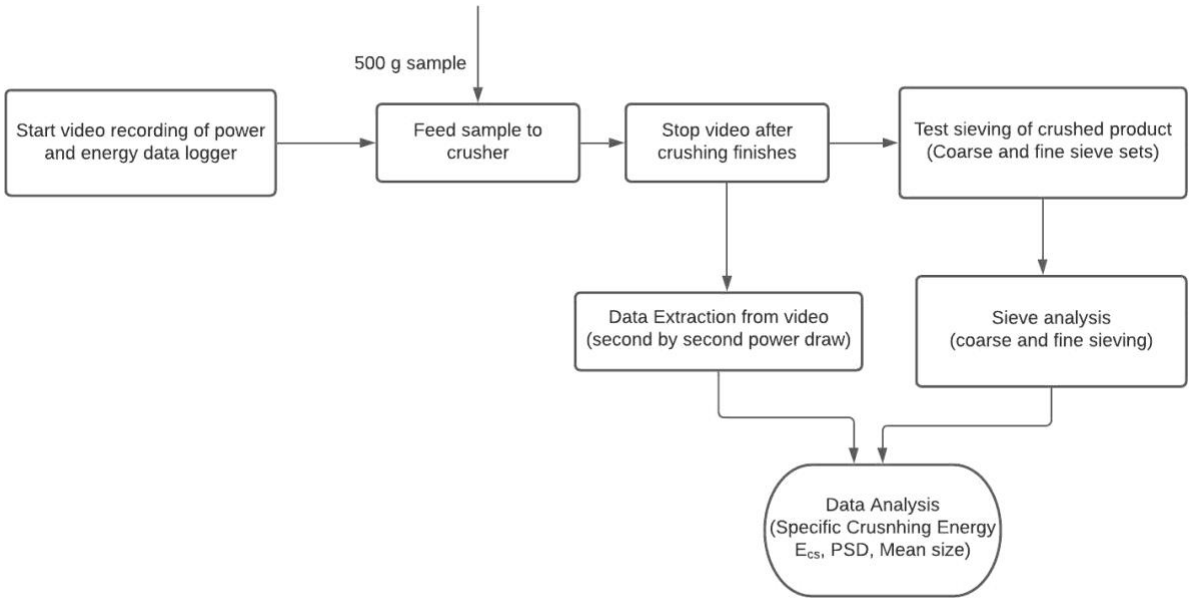

Figure 3-9 Experimental procedure for crushing of samples

Before putting the samples in the crusher, the non-loaded crusher power was recorded by a digital data logger, giving the power consumption of just the machine itself without any samples. This was done to get the idea of the machine's power consumption during the general running of machine parts that were not crushing. During the crushing of the samples, a video was made to record the changes in current, power and energy on the digital data logger. After the crushing finished, the crushed product was put in the ROTAP sieve shaker to carry out the sieve analysis.

The second-by-second data of power and energy from the video was extracted. The second-by-second power values from the digital data logger were then converted to second-by-second specific comminution energy (E_{cs}) in kWh/t. Then the cumulative specific comminution energy was calculated, adding all the values of each second. This process was done for both treated and non-treated samples. The calculations of one of the tests are shown in Appendix A. The cumulative E_{cs}

value of treated and nontreated samples was then compared and analyzed, which gave the results for impacts of MW on crushing energy.

Similarly, the data of PSD for both treated and non-treated samples were modelled using GGS and RR distribution model. The mathematical models obtained by plotting the PSD data were used to obtain the distribution parameter values, product critical sizes, and different size fractions. Finally, all the analyzing factors, i.e., E_{cs}, d_{50}, d_{80}, distribution parameter, ore loss (particles less than 1 mm and 300 µm) and circulating load (particles greater than 6mm) were measured in terms of % improvement by MW by using Equation 24.

$$\%\ \text{improvement by MW} = \frac{\text{Non} - \text{treated sample} - \text{Treated sample}}{\text{Non} - \text{treated}} * 100 \qquad (24)$$

Moreover, the percentage improvement per kWh/t of MW input was also analyzed to understand the feasibility of microwave application for processing.

4. Results and Discussion

In this chapter, the results of the impacts of microwave irradiation on HK kimberlite samples are presented. First, the impact of microwave power and input energy (exposure time) on product critical sizes (d_{50} and d_{80}) and the product size distribution parameter are evaluated. This is followed by the results of impacts of MW power and energy on the coarse and fine product fractions in terms of circulating load (% of particles greater than 6 mm), ore loss (particles less than 1 mm) and fine particles in tailings (% of particles less than 300 µm) are presented. In the end, the results for specific comminution energy E_{cs} during crushing in a single roll crusher are depicted and discussed. The results are the comparison between the microwave treated and non-treated samples of kimberlite.

4.1 Results of MW Impact on Product Critical Sizes and Distribution Parameter

4.1.1 Comparison of PSD Models

As described earlier, PSD models are based on equations. Those equations are used to get the data for cumulative passing % in the Gates Gaudin Schuhmann model or cumulative retained % in the Rosin Rammler model. The values obtained are then plotted on a log-log scale to get the plot. However, in this research, instead of using log-log scales, the log equations were used to get the values in terms of log and then plotted on a simple graph. The equations used are as follows.

$$\mathrm{Log}\left(\frac{\mathrm{W_P}}{100}\right) = \mathrm{mLog(x)} - \mathrm{mLog(k)} \quad \text{for GGS model} \tag{25}$$

$$\mathrm{Ln}\left[\mathrm{Ln}\left(\frac{100}{\mathrm{W_r}}\right)\right] = \mathrm{bLn(x)} - \mathrm{bLn(a)} \quad \text{for RR model} \tag{26}$$

The graph obtained by these equations was then used to get the model equation and R^2 value. One of the sample tables and graphs obtained by these equations is shown in Appendix C. The model equation can then be used to get the values of size and distribution parameters, which tells us about the coarseness and uniformity of product size distribution.

4.1.1.1 PSD Model for Coarse Size Fraction of Product (6700-1000 µm)

Table 4-1 shows the results obtained by plotting the graphs using the log values from the above equation. It can be seen that the R^2 value of the GGS model is much better and precise than the RR model. This tells us that the GGS model gave much better results and is suitable for this relatively coarser size fraction. Although the distribution parameter for the RR model is better than the GGS model, as the GGS model is precise based on R^2 value, the values of the distribution parameter obtained from the GGS model are considered.

Table 4-1: R^2 and distribution parameter values of GGS and RR model for coarse size fraction (6700 - 1000 µm)

	GGS Model		**RR Model**	
	R^2	**Distribution Parameter**	**R^2**	**Distribution Parameter**
Average	0.993	0.77	0.943	1.30
Maximum	0.997	0.88	0.961	1.36
Minimum	0.990	0.66	0.926	1.17
Std Dev	0.001	0.04	0.007	0.03
CV(%)	0.113	5.76	0.729	2.92

Figure 4-1 tells us about the error in values predicted by both models. It can be seen that the error in the mass fraction values predicted by the GGS model to the original mass fraction values (obtained by sieve analysis) is much less as compared to the RR model. So, it can be said that the GGS model is overall better than the RR model. This is in line with for which these models were developed in the first place. Furthermore, the GGS model is preferred for the processing of minerals (Barry A. Wills et al., 2016a) and relatively coarser size fraction. So, in this case, GGS gave better results as the size fraction was coarser, which aligns with the literature work.

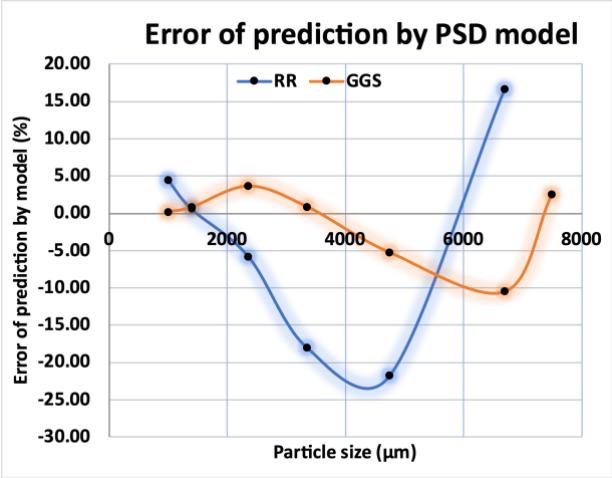

Figure 4-1 Error prediction by PSD models for coarse size fraction

4.1.1.2 PSD Model for Fine Size Fraction of Crushed Product (850-53 µm)

Table 4-2 shows the results obtained by plotting the graphs using the log values from the above equation. The R^2 value of the RR model is slightly better than the GGS model but the error in the mass fraction values predicted by the RR model to the original mass fraction values (obtained by sieve analysis) is still high, especially for the larger particle size. This indicates that for a fine particle size fraction, the RR model can be used, but as the error of the RR model increases, the values obtained from the GGS model are considered to be more reliable and are taken for the results of MW impacts.

Table 4-2: R^2 and distribution parameter values of the GGS and the RR model for fine size fraction (850 - 53 µm)

	GGS Model		**RR Model**	
	R^2	**Distribution Parameter**	**R^2**	**Distribution Parameter**
Average	0.989	0.74	0.992	1.02
Maximum	0.994	0.77	0.993	1.05
Minimum	0.985	0.70	0.990	0.99
Std Dev	0.003	0.02	0.001	0.01
CV(%)	0.269	2.76	0.092	1.71

Figure 4-2 tells us about the error in values predicted by both models. It can be seen that the error % for both models are not far from each other. The error in values predicted by the RR model is less when we move towards finer particle size. The error in values predicted by GGS becomes less as we move towards coarser particle size. This is in line with for which these models were developed in the first place. The RR model was developed for minerals, especially coal and relatively finer size fractions (Gupta & Yan, 2016) (Barry A. Wills et al., 2016a). The same was observed in this study as well that for finer size fractions of ore, the RR model gave the better results.

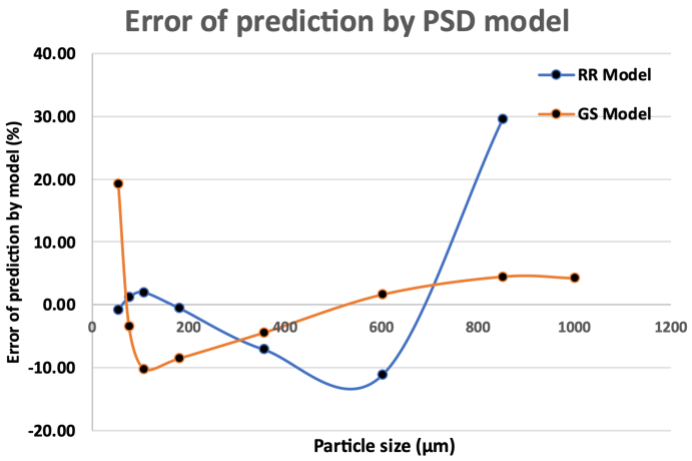

Figure 4-2 Error prediction by PSD models for fine size fraction

For this research work, the GGS model is considered the better model, and the values obtained by the GGS model are considered to comprehend the results obtained by the effect of MW.

4.1.2 Impact of MW on Product Critical Sizes and Distribution Parameter

The 500 g samples of HK kimberlite samples were screened after crushing. The values obtained from the screening were put in the GGS model to ascertain the results of evaluating factors like d_{50} and d_{80}. The critical sizes and distribution parameter results at different power levels and energy are discussed in the following paragraphs.

4.1.2.1 Power 15 kW

The results of improvement due to MW irradiations in critical sizes of d_{50} and d_{80} and the product distribution parameter of samples treated at the power of 15 kW and energy level ranging from around 8 kWh/t to 150 kWh/t are shown in Figure 4-3. It is evident that the mean critical size of d_{50} and d_{80} and the distribution parameter improved positively compared to non-treated samples, especially at low energy levels. The improvement in distribution parameter and d_{50} at an energy level of around 8 kWh/t improved to around 15 and 18%, respectively. Moreover, the improvement in d_{80} size was not that high but still at low energy levels; the improvement achieved was up to 6%. However, the improvement in these factors follows a decreasing trend with an increase in energy levels. At higher energy levels, the negative effect of the impact of MW irradiations was obtained. This means that at higher energy levels, the critical sizes of d_{50}, d_{80} and distribution parameters were low compared to non-treated kimberlite samples. This negative effect even reached -4%.

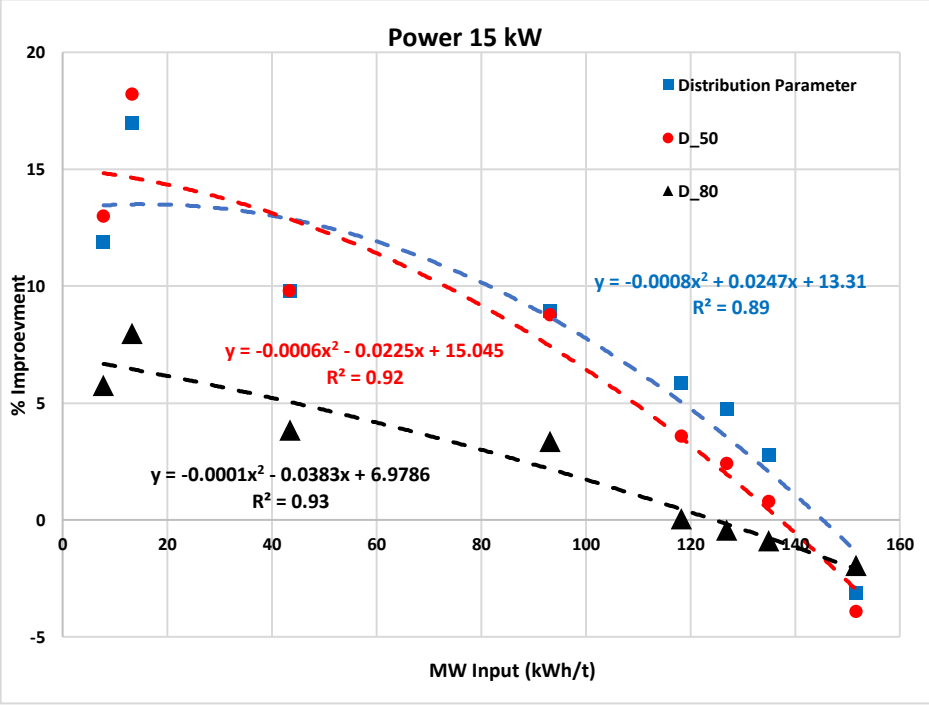

Figure 4-3 Percentage improvement in product mean size and distribution parameter by MW input at 15 kW power

Figure 4-4 shows the effect of improvement per kWh/t of MW input in critical sizes and distribution parameters at the power of 15 kW. The results show that lower energy levels range (up to 40 kWh/t) is the efficient and feasible range of using MW irradiations which render optimum results in improvement of critical size. On the other hand, higher energy levels are not adequate and will even lead to negative impacts.

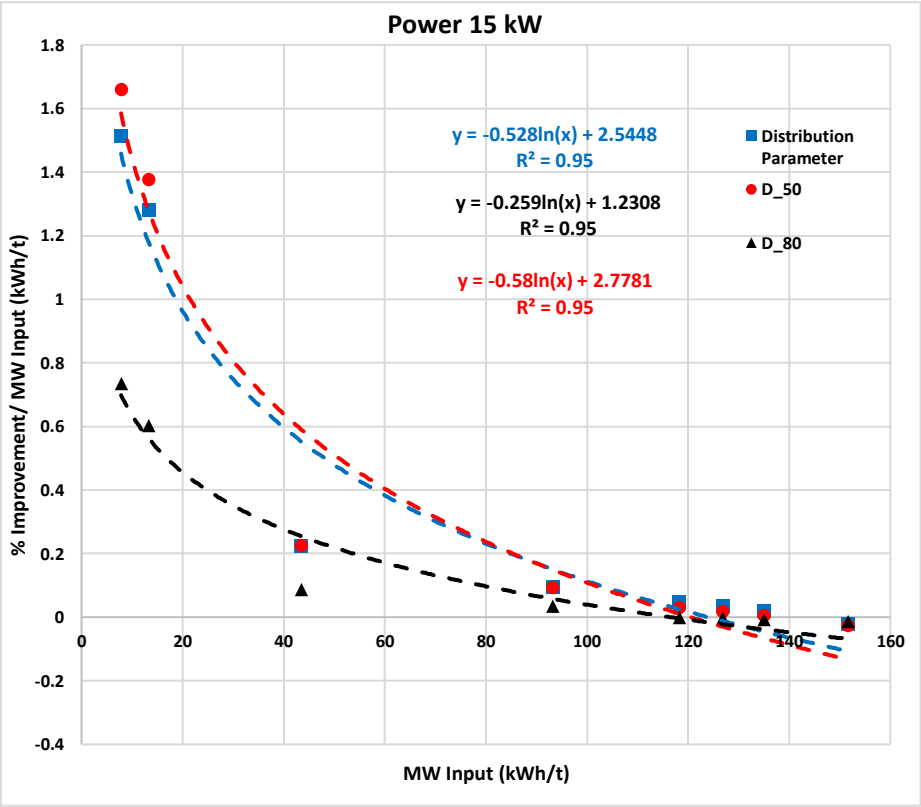

Figure 4-4 Percentage improvement per kWh/t of MW input in the product mean size and distribution parameter by MW input at 15 kW power

4.1.2.2 Power 10 kW

Figure 4-5 depicts the experimental results obtained for critical sizes and distribution parameters at a power of 10 kW in terms of improvement percentage due to MW irradiations. The graph shows that the trend of the results obtained at 10 kW is similar to that achieved at 15 kW. The critical size of d_{50} and d_{80} and the distribution parameter improved compared to non-treated samples. The improvement in distribution parameter and d_{50} at the energy level of around 8 kWh/t improved up to around 8%. However, this improvement was 30-40% less as achieved at a power of 15 kW.

Similarly, the improvement in d_{80} size was around 4.5%, which was around 20% less than achieved at 15 kW.

The trend for improvement decreased with the increase in energy level. At a power of 10 kW, the d_{50} and product size distribution stayed positive, and no adverse effect was observed. This means that at lower power, the improvement in these factors regressed but stayed towards a positive impact. But the critical size of d_{80} still depicted the negative impacts at higher energy levels.

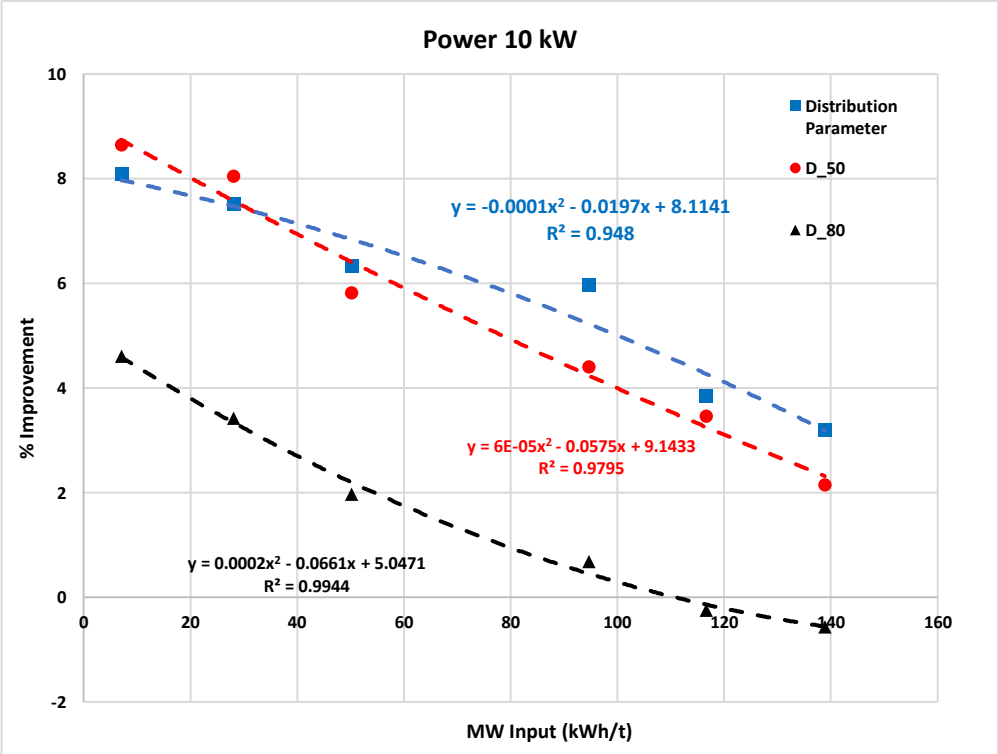

Figure 4-5 Percentage improvement in the product mean size and distribution parameter by MW input at 10 kW power

Figure 4-6 shows the effect of improvement per kWh/t of MW input in critical sizes and distribution parameters at the power of 10 kW. The trend in improvement per kWh/t is again similar to the one obtained at the power of 15 kW. The lower energy levels range is the proficient way of using MW irradiations which render best results in improvement of critical size. Higher energy levels are not at all adequate and will lead to negative impacts.

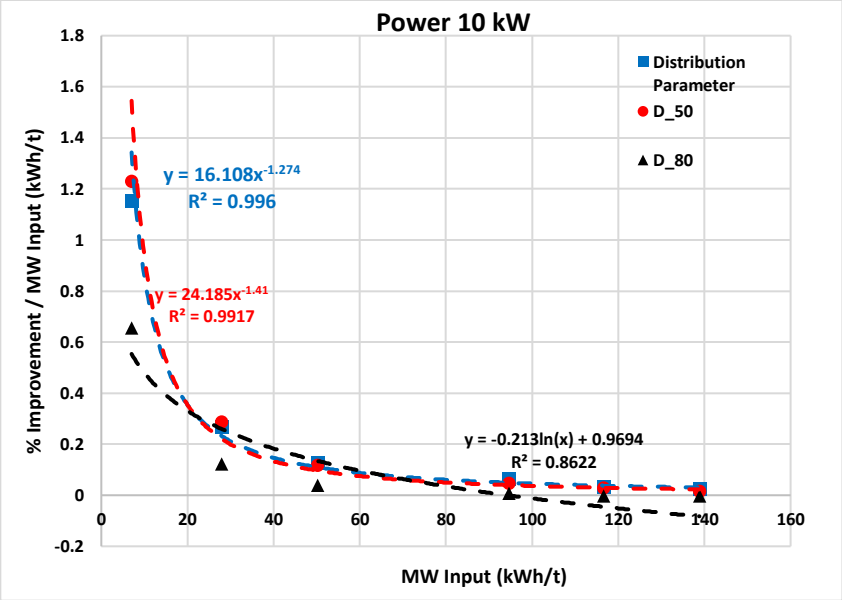

Figure 4-6 Percentage improvement per kWh/t of MW input in the product mean size and distribution parameter by MW input at 10 kW power

4.1.2.3 Power 5 kW

To see the effects of lower MW power irradiations on kimberlite samples, several tests were conducted at a power of 5 kW with the energy level ranging from 30 – 150 kWh/t. The findings of these experiments are shown in Figure 4-7. The improvement in the product size distribution and critical sizes of d_{50} and d_{80} can be seen compared to the non-treated kimberlite samples. The improvement in distribution parameter and d_{50} at an energy level of around 30 kWh/t improved up to around 6 and 5%, respectively. Moreover, the improvement in d_{80} size was not significant and was close to 1%.

Similar to the results of Power of 15 and 10 kW, the improvement in these factors follows a decreasing trend with the increase of energy levels. With a power of 5 kW, the d_{50} and product size distribution decreased, but still, the impact was towards the positive side, and it still showed improvement compared to the non-treated samples. However, this improvement is not a lot and is close to being negligible. Nevertheless, the critical size of d_{80} still depicted the negative impacts at higher energy levels.

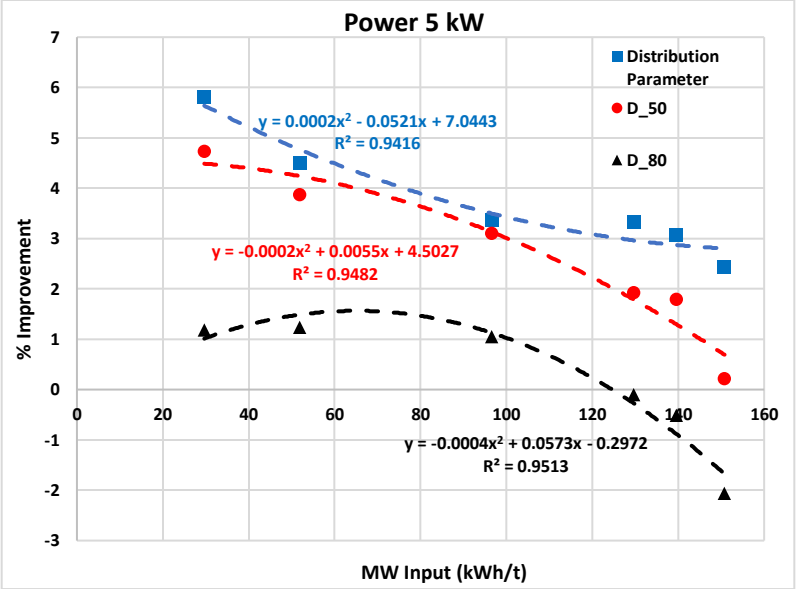

Figure 4-8 Percentage improvement in the product mean size and distribution parameter by MW input at 5 kW power

The results obtained for improvement per MW Input (kWh/t) are shown in Figure 4-8. The results illustrate the same trend as was obtained for higher power levels. The results show that a lower energy level range (no higher than 40 kWh/t) is the economical way of using MW irradiations which render optimum results in improvement of critical size. Higher energy levels will lead to inefficient use of MW and may not even be positive in terms of increasing the critical size of the product.

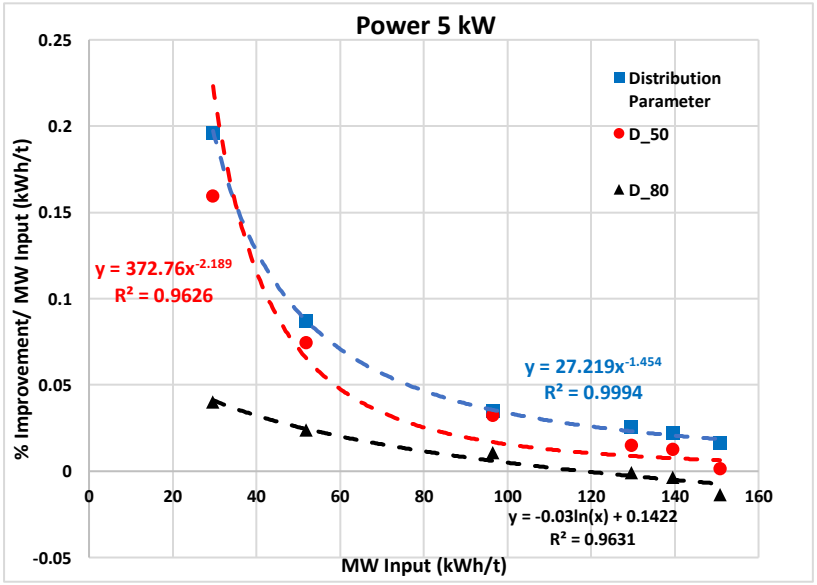

Figure 4-7 Analysis on the results of MW Impact on Product Mean Size

These MW irradiations on kimberlite samples increased the particles' average surface temperature, which induced the inter-granular cracks. The same was also observed in the studies on kimberlite by Deyab et al. (2021) and Kobusheshe (2010). These inter-granular cracks increased the product critical sizes, which is in line with one of the predictions of the study conducted by Walkiewicz in which it was stated that the microwaves have the potential of better liberation at higher particle d_{80} (John W Walkiewicz et al., 1991). However, this improvement in product critical sizes decreased with the increase of microwave energy because the particles absorbed more energy and got heated, resulting in more intergranular cracks generation. This was observed as well in the study by (Crane et al., 2014). This led to the liberation of finer particles, resulting in the finer fraction and bringing down the value of the critical size.

The improvement per kWh/t in product critical size is achieveable and can lead to positive economic impact only if the exposure of MW is kept to short exposures with a high-power level. These obtained results show that this improvement trend decreases with increasing energy level, which makes MW use uneconomical and inefficient in the case of increasing product critical sizes. In one of the studies, Kingman also concluded that short exposure of MW on rocks could positively impact (Kingman & Rowson, 1998).

4.2 Results of MW Impact on Ore Loss and Circulation Load

The evaluation of critical sizes was followed by analyzing the effects of MW on the ore loss and circulating load. First, the ore loss was evaluated by checking the percentage of particles less than 1 mm and 300 µm. Second, the effect of circulating load was examined by assessing the percentage of particles greater than 6 mm. The results of these parameters at different power levels and energy are discussed in the following paragraphs.

4.2.1 Power 15 kW

The samples treated at a power of 15 kW were evaluated in terms of the percentage of particles less than 1 mm and 300 µm and the percentage of particles greater than 6 mm. The results of percentage improvement due to MW irradiations in these parameters are shown in Figure 4-9. The results obtained illustrate that the percentage of ore loss was reduced to a value of about 25% compared to non -treated samples. Similarly, the percentage of particles less than 300 µm was

reduced to around 10 %. However, this improvement followed a decreasing trend with the increase of energy and even reached a negative impact at a higher energy level.

The percentage of particles greater than 6 mm representing the circulating load was more at the lower energy level, which is a negative impact of MW on circulation load. However, this parameter observed an increasing trend with an increase in the energy level, which means that with the increase of energy input by MW, the circulating load was reduced.

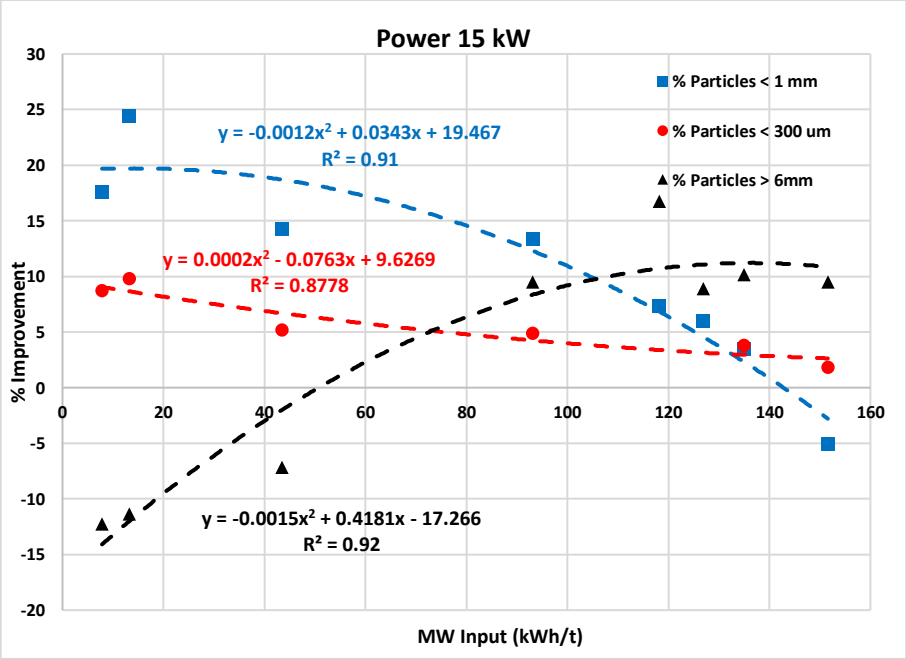

Figure 4-9 : Percentage improvement in ore loss and circulating load by MW input at 15 kW power

Figure 4-10 presents the data of improvement per kWh/t of MW input. It can be observed from the graphs that the improvement followed a decreasing trend with the increase of MW input for the parameters of ore loss. This indicates that better improvement can be achieved at lower MW input which will be cost-effective. However, in the case of circulating load, the trend indicates that to achieve better results in terms of circulating load, more MW input is the right way forward. This is because more exposure to MW irradiations can improve the circulation load, which means fewer particles will be greater than 6 mm and avoid over-crushing, leading to a reduction in the potential of diamond breakage.

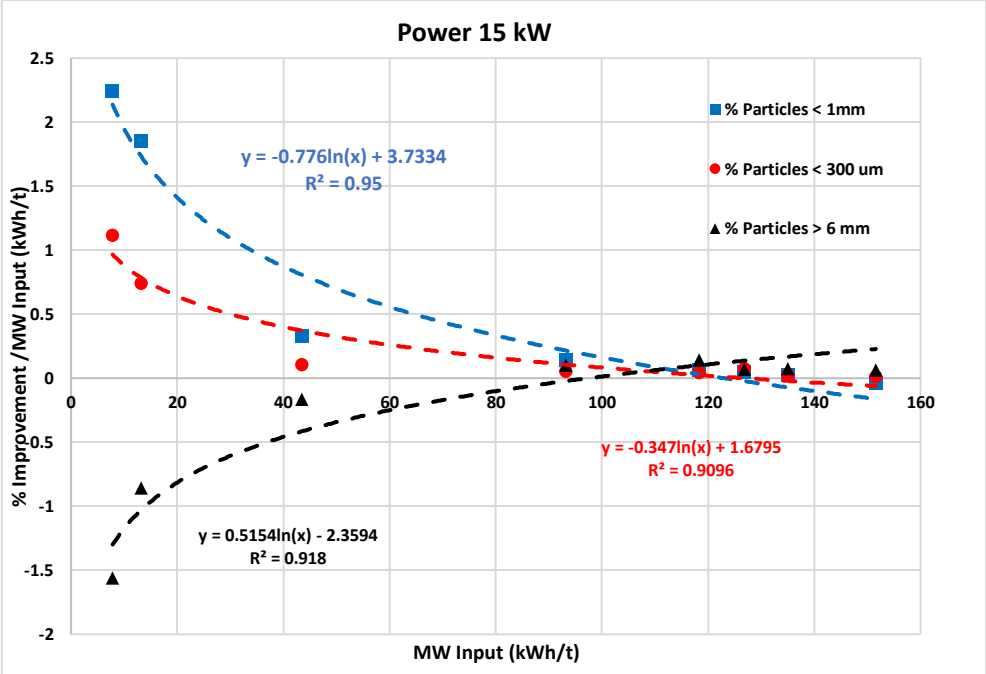

Figure 4-10 Percentage improvement per kWh/t of MW input in ore loss and circulating load by MW input at 15 kW power

4.2.2 Power 10 kW

The effects of MW irradiations at a power of 10 kW on ore loss and circulating load are presented in Figure 4-11. The results of improvement due to MW irradiations portrays that the percentage of ore loss (particles less than 1 mm) was reduced up to the value of about 12%, whereas the percentage of particles less than 300 µm were reduced to around 8.5% as compared to non -treated samples. The overall trend obtained in these parameters was almost the same as the one obtained at 15 k W, i.e., the improvement reduced with increasing the energy level. However, this reduction did not reach any negative impact and stayed towards the improvement.

The improvement in circulating load was negative in the lower energy levels but reached around 9% at the energy of 140 kWh/t, which showed the increasing trend with increasing energy levels.

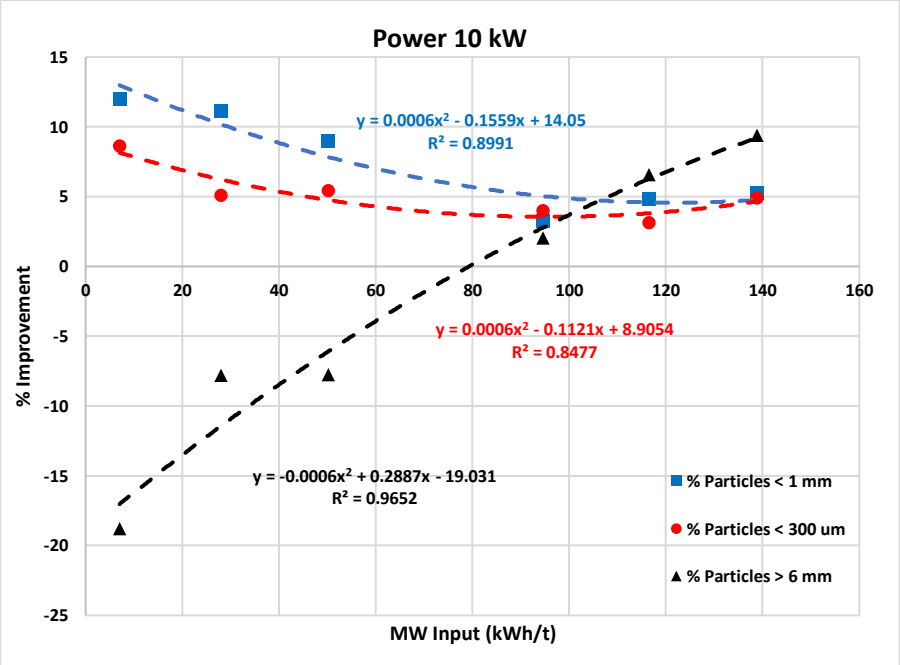

Figure 4-11 Percentage improvement in ore loss and circulating load by MW input at 10 kW power

If we consider the factor of improvement with MW Input, the results are presented in Figure 4-12. The trend observed is the same as for 15 kW, which tells us that the optimum improvement can be achieved at lower MW input levels for ore loss, but in the case of circulating load, the better results are available at, the higher MW input levels.

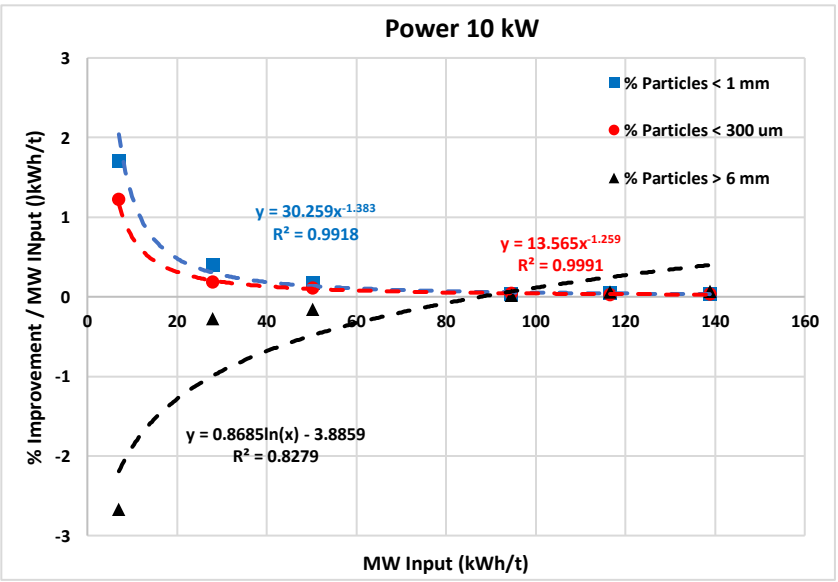

Figure 4-12 Percentage improvement per kWh/t of MW input in ore loss and circulating load by MW input at 10 kW power

4.2.3 Power 5 kW

The outcomes of MW irradiations at a power of 5 kW on ore loss and circulating load are presented in Figure 4-13. The results of improvement reveal that the percentage of ore loss (particles less than 1 mm) was reduced by nearly 8%, whereas the percentage of particles less than 300 µm was reduced to around 5 % compared to non -treated samples. The overall trend obtained in the percentage of particles less than 1 mm was almost the same as obtained at higher power levels, i.e., the improvement reduced with increasing the energy level, and this reduction did not reach the negative levels. In the case of the percentage of particles less than 300 µm, the trend was slightly different at 5 kW compared to 10 and 15 kW. However, it almost stayed constant, and some increase was observed at the higher energy levels.

Moreover, the improvement in circulating load was only -2 % in the lower energy levels, and an inclined increase was observed with the increase of energy. The improvement in circulating load even reached 12 %, which was not observed at the power of 10 and 15 kW.

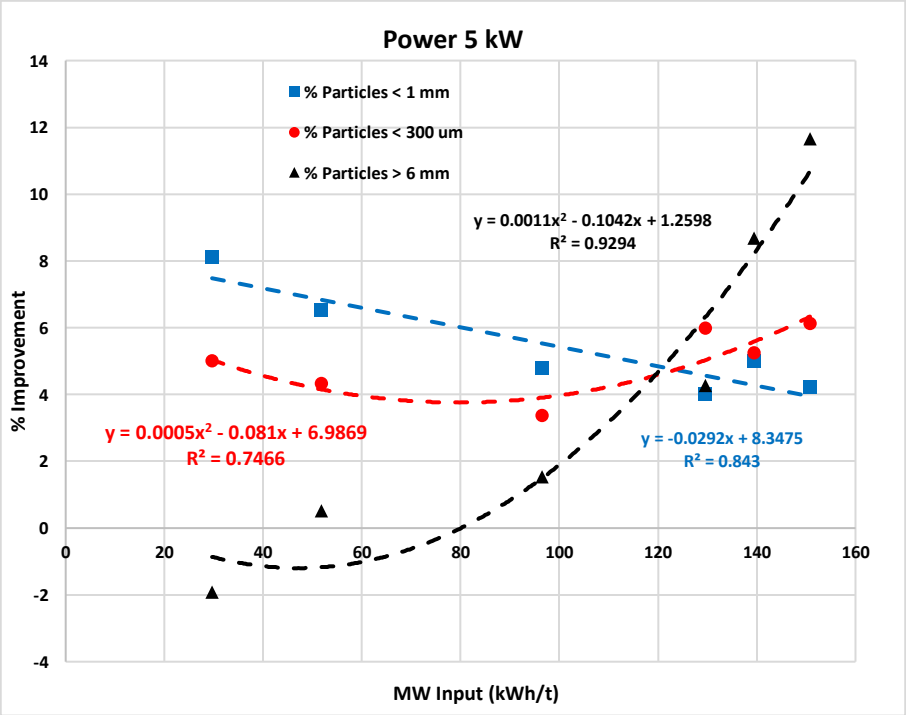

Figure 4-13 Percentage improvement in ore loss and circulating load by MW input at 5 kW power

If we consider improvement per MW Input, the results are presented in Figure 4-14. The increasing trend is observed for circulating load improvement with microwave input, but for ore loss, the optimal conditions are to use lower MW energy levels which will be an efficient way of using MW irradiations.

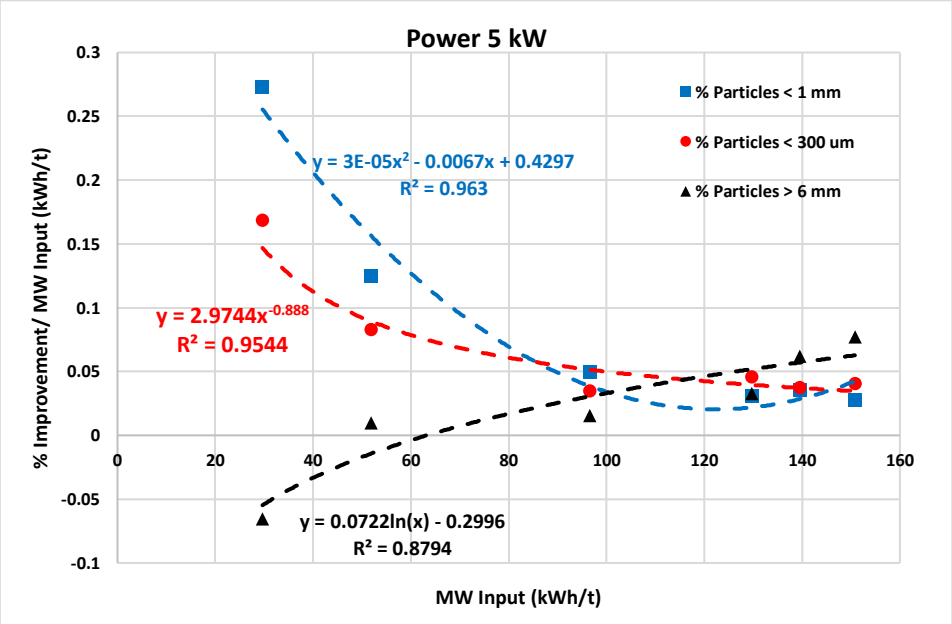

Figure 4-14 Percentage improvement per kWh/t of MW input in ore loss and circulating load by MW input at 5 kW power

4.2.3.1 Analysis of the results of MW Impact on Ore loss and Circulating Load

As discussed above, the MW irradiations on kimberlite samples increased the particles' average surface temperature, which induced the inter-granular cracks. These inter-granular cracks resulted in better liberation during crushing and increased the fraction of particles greater than 6 mm, 1mm and 300 µm. A larger fraction of particles greater than 1mm and 300 µm means a reduction in ore loss which is a positive impact of microwave on kimberlite processing. However, an increase in the fraction of particles greater than 6 mm is not a good sign as it will increase the circulating load, which negatively impacts kimberlite processing. This is because the improvement in % of ore loss follows a decreasing trend with the increase in microwave energy. Nevertheless, the percentage of circulating load improvement follows an increasing trend with the increase in microwave energy. The same trend was observed in a similar research conducted by Kumar et al. on iron ore

grindability improvement in which there was an improvement in the percentage of particles greater than 750 µm by microwave treatment, but it decreased with more exposure to microwave irradiations (Kumar et al., 2010). This decrease in the improvement of particles less than 1 mm and 300 µm and improvement of particles greater than 6 mm with the increase of microwave energy is because the particles absorbed more energy and got heated, resulting in more intergranular cracks generation.

The results obtained for ore loss and circulating load were similar to those obtained for product critical sizes in terms of % improvement per kWh/t. This means that MWs can be used efficiently and can be proficient in terms of economic values if materials are exposed for a short period of time. On the other hand, the higher exposure time of MW will not show much improvement and will be uneconomical and negatively impact ore loss and circulating load. This is in line with the studies carried out by Kingman, which gave a similar suggestion that using MW for short exposure time can be beneficial (Kingman & Rowson, 1998).

4.3 Results of MW Impact on Specific Comminution Energy

The energy consumed during crushing of kimberlite was measured in terms of E_{cs} per kWh/t and evaluated to compare the treated and non-treated samples of kimberlite. The results obtained are discussed in the following paragraphs.

The averaged E_{cs} value for non-treated kimberlite samples was around 2.778 kWh/t. The results for treated samples at 15-, 10- and 5-kW power levels are shown in Figure 4-15. It can be seen from the graph that the E_{cs} of treated samples were significantly below to that of non-treated samples. The reduction in E_{cs} increased with increasing both input power and energy levels. However, at energy levels of around 270 kJ (150 kWh/t), a slight change was observed. Although there was still an improvement from non-treated sample values, a reduction in E_{cs} slightly regressed compared to the previous energy level of 250 kJ.

The results in terms of improvement can be seen in Figure 4-16. E_{cs} reduction improved up to 16%, 11.5% and around 9% with the power of 15-, 10- and 5-kW MW powers. An increasing trend in improvement was observed with the increase of power and energy levels which depict that with

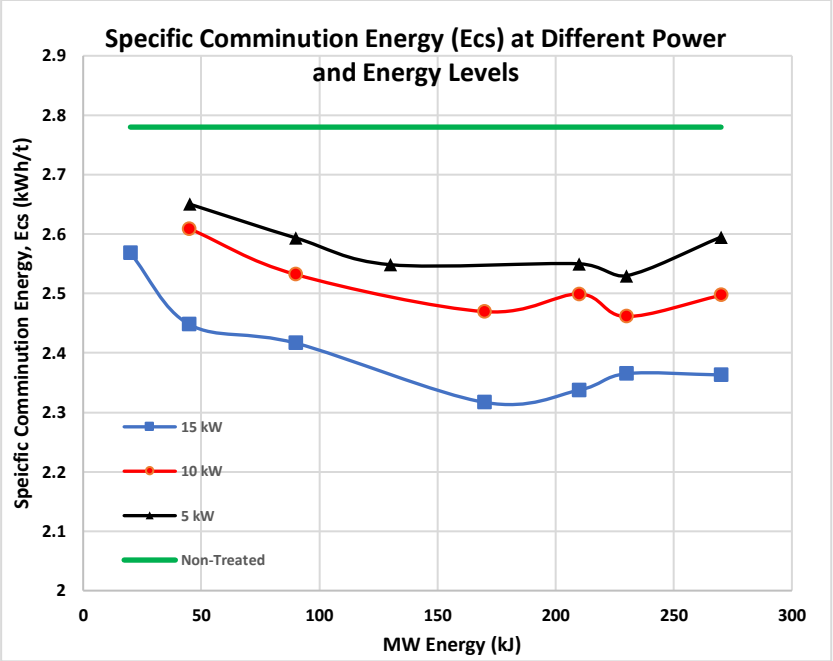

Figure 4-15 Comparison of specific comminution energy (E_{cs}) of MW treated and non-treated samples

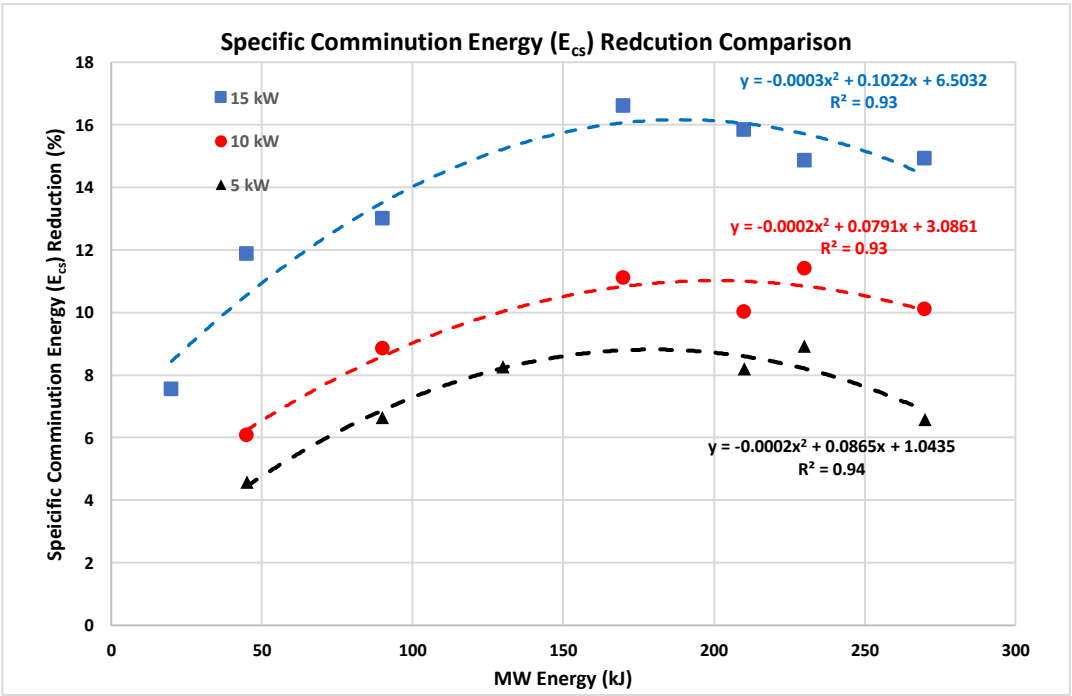

Figure 4-16 Percentage improvement in specific comminution energy (E_{cs}) by MW input at different power levels

more energy and power induced by microwave, more cracks in the kimberlite samples occur. This crack generation resultantly reduced the strength of kimberlite ore material. The same observation was reported by the work conducted on kimberlite (Deyab et al., 2021) (Kobusheshe, 2010).

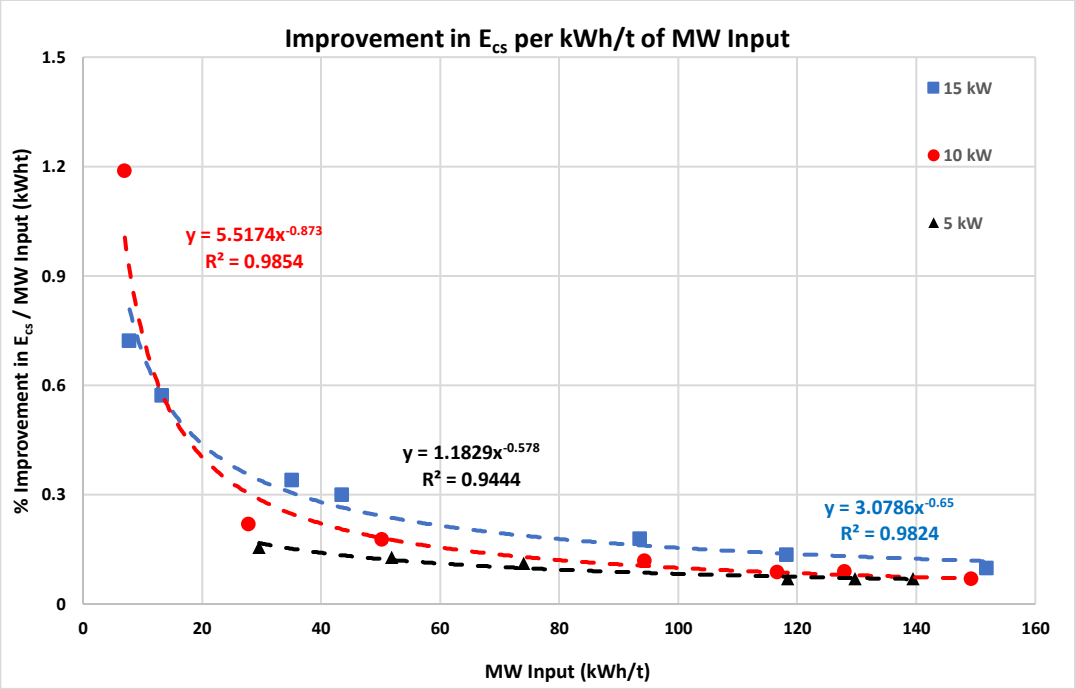

Figure 4-17 Improvement per kWh/t of MW input in specific comminution energy (E_{cs}) by MW input at different power levels

Consequently, the reduction in the strength of kimberlite samples led to the reduction of E_{cs} value compared to the non-treated samples during the crushing of samples in a single roll crusher.

If we take into account the effect of improvement per MW Input (kWh/t), the results are illustrated in Figure 4-17. It is observed that the most effective and optimum use of MW irradiations in E_{cs} reduction is observed by using low energy levels but higher power. Even using low power at a lower energy level is seen to be the effective way of using MW irradiations to reduce E_{cs} during the crushing stage of processing. However, the improvement per MW input for E_{cs} at higher energy levels was not that significant compared to improvement at lower energy levels. Due to this low increase in improvement at higher levels, the MW irradiations on kimberlite are not that efficient and will not be economically feasible to be used at higher levels.

5. Conclusion and Scope for Future Work

5.1 Conclusions

The research work in this thesis covers the study of impacts of microwave irradiations on crushing of kimberlite ore samples while considering the product critical size, ore loss (particles less than 1 mm and 300 µm), circulating load (particles greater than 6 mm) and specific comminution energy, E_{cs} as the criteria for evaluation. A commercial high-power microwave system with the capability of working up to the power of 15 kW and a frequency of 2.45 GHz was used as a single-mode microwave cavity system. The input energy levels of up to 270 kJ were used to irradiate 500 g crushed kimberlite samples ranging in size from 16 to 31.5 mm. The samples were crushed using a single roll crusher and then screened to get the product size distribution. The conclusions resulting from this thesis are discussed in the following paragraphs.

5.1.1 Effect of MW on Critical Sizes

- The MW irradiations showed improvement in increasing the critical sizes of d_{50} and d_{80} of the crushed product.
- The improvement in critical size was maximum at lower energy levels at all the power of 5, 10 and 15 kW. However, the reduction in the improvement % was observed with the increase in the energy level.
- In the case of higher power of 15 kW, even negative impact of MW irradiations was observed at high energy levels, which means that the critical sizes of d_{50} and d_{80} of the crushed product were decreased compared to non-treated samples of kimberlite ore.
- The optimum results in terms of critical size can be achieved by using the MW at high power, i.e., 15 kW but lower energy levels (short exposure time).

5.1.2 Effect of MW on Ore Loss and Circulation Load

- The impact of MW irradiations on ore loss revealed improvement in reducing the ore loss of the crushed product.
- The reduction in ore loss regressed with the increase in MW energy level.

- For circulating load, i.e., particles greater than 6 mm, the negative effect was seen at the lower energy levels at all the power levels. However, this negative effect was reduced with increased energy levels and even reached a positive effect at higher energy levels.
- The % improvement in ore loss reduction was maximum at lower energy levels at all the power of 5, 10 and 15 kW.
- In the case of higher power of 15 kW, the negative impact of MW irradiations was observed for ore loss, and it reached the value of around -5 % at the MW input of around 150 kWh/t.
- The optimum results in ore loss reduction can be achieved by using the MW at high power, i.e., 15 kW but with lower energy levels.
- The reduction in circulating load can be optimized by using the lower power level (5 kW) and increasing the energy level.

5.1.3 Effect of MW on Comminution Energy Consumption

- The MW irradiations reduced the specific comminution energy E_{cs} of treated samples.
- The improvement in reduction of E_{cs} was a maximum of around 16 % at the power of 15 kW.
- The improvement in E_{cs} reduction followed an increasing trend with the increase in MW energy level.
- The improvement was observed for all the power levels, i.e., 5, 10 and 15 kW.
- A slight reduction in the improvement % was observed at the highest energy level of MW energy input.
- The optimum results in E_{cs} reduction per kWh/t of MW input can be obtained at lower energy levels, which will be cost-effective and energy-efficient.

5.2 Scope for Future Work

The study on the effect of microwave-assisted crushing appears to be feasible and can be used practically during the processing of kimberlite ores.

- Conduct a study on the impact of MW irradiations on downstream processing operations like dense media separation to see the effect of MW on separating ore minerals from gangue material.

- Investigate the influence of MW on crushing by analyzing the effects on breakage functions to acquire knowledge on production rate.
- Examine the effect of MW on different size fractions and mass of crushed sample to check the efficacy of microwave on strength reduction.
- The recommended studies can be combined to make an optimized multi-variable microwave-assisted processing system, which can further help to study the cost-effectiveness of microwaves application in the kimberlite processing.

References

Adl-Zarrabi, B. (2006). Forsmark site investigation - Thermal properties of rocks using calorimeter and TPS method.

Al-Harahsheh, M., Kingman, S., Saeid, A., Robinson, J., Dimitrakis, G., & Alnawafleh, H. (2009). Dielectric properties of Jordanian oil shales. *Fuel Processing Technology*, *90*(10).

Austin, L. G., Klimpel, R. R., & Luckie, P. T. (1984). Process engineering of size reduction: ball milling. In *Process Eng of Size Reduction, Ball Milling*.

Bond, F. (1961). Crushing and Grinding calculations. *British Chemical Engineering*, *6*.

Boone Beck, D. M. (2016). Applicability of Hydraulic Borehole Mining ('Hbhm') to Diamondiferous Deposits. *Angewandte Chemie International Edition, 6(11), 951–952.*

Chen, T. T., Dutrizac, J. E., Haque, K. E., Wyslouzil, W., & Kashyap, S. (1984). The relative transparency of minerals to microwave radiation. *Canadian Metallurgical Quarterly*, *23*(3).

Church, R. H., Webb, W. E., & Salsman, J. B. (1988). Dielectric properties of low-loss minerals. In *Report of Investigations - United States, Bureau of Mines* (Issue 9194).

Collin, R. E. (2010). Foundations for Microwave Engineering. In *Foundations for Microwave Engineering*.

Crane, C. A., Pantoya, M. L., Weeks, B. L., & Saed, M. (2014). The effects of particle size on microwave heating of metal and metal oxide powders. *Powder Technology*, *256*.

Deyab, S. M., Rafezi, H., Hassani, F., Kermani, M., & Sasmito, A. P. (2021). Experimental investigation on the effects of microwave irradiation on kimberlite and granite rocks. *Journal of Rock Mechanics and Geotechnical Engineering*, *13*(2).

Dutta, T., Kim, K. H., Uchimiya, M., Kwon, E. E., Jeon, B. H., Deep, A., & Yun, S. T. (2016). Global demand for rare earth resources and strategies for green mining. In *Environmental Research* (Vol. 150).

Erlich, E. I., & Dan Hausel, W. (2002). *Diamond Deposits*.

Fitzgibbon, K. E., & Veasey, T. J. (1990). Thermally assisted liberation - a review. *Minerals Engineering*, *3*(1–2).

Fuerstenau, D. W., & Abouzeid, A. Z. (2002). The energy efficiency of ball milling in comminution. *International Journal of Mineral Processing*, *67*(1–4).

Gabriel, C., Gabriel, S., Grant, E. H., Halstead, B. S. J., & Michael P Mingos, D. (1998). Dielectric parameters relevant to microwave dielectric heating. *Chemical Society Reviews*, *27*(3).

Griffiths, D. J., & Inglefield, C. (2005).Introduction to Electrodynamics. *American Journal of Physics*, *73*(6).

Güngör, A., & Atalay, Ü. (1998). Microwave Processing and Grindability. *7th International Mineral Processing Symposium*.

Guo, S. H., Chen, G., Peng, J. H., Chen, J., Li, D. B., & Liu, L. J. (2011). Microwave assisted grinding of ilmenite ore. *Transactions of Nonferrous Metals Society of China (English Edition)*, *21*(9).

Gupta, A., & Yan, D. (2016). Mineral Processing Design and Operations: An Introduction: Second Edition. In *Mineral Processing Design and Operations: An Introduction: Second Edition*.

Haldar, S.K. (2013). Mineral Processing. *Mineral Exploration*, 223–250.

Haldar, Swapan K. (2018). Mineral Exploration Principles and Applications. In *Economic Geology* (Vol. 108, Issue 6).

Haque, K. E. (1999). Microwave energy for mineral treatment processes - A brief review. *International Journal of Mineral Processing*, *57*(1).

Harlow, G. . (1998). The Nature of diamonds. *Choice Reviews Online*, *35*(08).

Hassani, F., Shadi, A., Rafezi, H., Sasmito, A. P., & Ghoreishi-Madiseh, S. A. (2020). Energy analysis of the effectiveness of microwave-assisted fragmentation. *Minerals Engineering*, *159*(June), 106642.

Hodgson, I. M. J. (1981). The Hydrothermal Alteration of Kimberlite. *Thesis in Fulfillment of Degree of Doctor of Philosophy. Department of Mineral Resource Engineering*, *December*.

Holman, B. W. (1926). Heat treatment as an agent in rock breaking. *Transactions of the Institute of Mining and Metallurgy*.

King, R. P. (2001). Comminution operations. In *Modeling and Simulation of Mineral Processing Systems*.

King, R. P., & Schneider, C. L. (1998). Mineral liberation and the batch comminution equation. *Minerals Engineering*, *11*(12).

Kingman, S. W. (2006). Recent developments in microwave processing of minerals. *International Materials Reviews*, *51*(1).

Kingman, S. W., & Rowson, N. A. (1998). Microwave treatment of minerals - A review. *Minerals Engineering*, *11*(11).

Kingman, S. W., Vorster, W., & Rowson, N. A. (2000). Influence of mineralogy on microwave

assisted grinding. *Minerals Engineering*, *13*(3).

Kobusheshe, J. (2010). *Microwave enhanced processing of ores. PhD thesis, University of Nottingham.*

Kumar, P., Sahoo, B. K., De, S., Kar, D. D., Chakraborty, S., & Meikap, B. C. (2010). Iron ore grindability improvement by microwave pre-treatment. *Journal of Industrial and Engineering Chemistry*, *16*(5), 805–812.

Maurice, N.; Kenneth, C. (2003). Principles of Mineral Processing. *SME*.

Meredith, R. (1998). Engineers' Handbook of Industrial Microwave Heating. In *Engineers' Handbook of Industrial Microwave Heating*.

Metso, Sandgren, E., Berglinz, B., & Modigh, S. (2015). *Basics in Mineral Processing Handbook*.

Mita, J. N. (2018). *The Effect of Microwave Irradiation on the Physicochemical Properties of Pyrite*. *April*.

Morkel, J. (2006). *Kimberlite Weathering : Mineralogy and Mechanism*.

Motlagh, P. N. (2009). *An investigation on the influence of microwave energy on basic mechanical properties of hard rocks*.

Nadolski, S., Klein, B., Kumar, A., & Davaanyam, Z. (2014). An energy benchmarking model for mineral comminution. *Minerals Engineering*.

Napier-Munn, T. (2015). Is progress in energy-efficient comminution doomed? *Minerals Engineering*, *73*.

Napier-Munn, T. J., Morrell, S., Morrison, R. D., & Kojovic, T. (1996). Mineral comminution

circuits: Their operation and optimisation. In *Julius Kruttschnitt Mineral Research Centre*.

Norgate, T., & Haque, N. (2010). Energy and greenhouse gas impacts of mining and mineral processing operations. *Journal of Cleaner Production*, *18*(3).

Pierson, H. O. (1993). Structure and Properties of Diamond and Diamond Polytypes. *Handbook of Carbon, Graphite, Diamonds and Fullerenes*, 244–277.

Pozar, D. (2005). Microwave Engineering Fourth Edition. In *Zhurnal Eksperimental'noi i Teoreticheskoi Fiziki*.

Rosin, P., & Rammler, E. (1933). *Laws governing the fineness of powdered coal*.

Sahyoun, C., Kingman, S. W., & Rowson, N. A. (2004). High powered microwave treatment of carbonate copper ore. *European Journal of Mineral Processing and Environmental Protection*, *4*(3).

Saxena, A. . (2009). *Electromagnetic Theory and Applications* (1st editio). Alpha Science Intl Ltd.

Schönert, K. (1988). A first survey of grinding with high-compression roller mills. *International Journal of Mineral Processing*.

Schuhmann, Jr., R. (1940). Principles of Comminution. I - Size Distribution and Surface Calculations. In *Mining Technology*.

Smith, R. . (1984). *Microwave power in industry*.

Vorster, W. (2001). The Effect of Microwave Radiation on Mineral Processing. *Chemical Engineering*, *June*.

Walkiewicz, J. W., Kazonich, G., & McGill, S. L. (1988). Microwave heating characteristics of

selected minerals and compounds. *Minerals and Metallurgical Processing*.

Walkiewicz, John W, Clark, A. E., & Mcgill, S. L. (1991). Microwave-Assisted Grinding. *IEEE Transactions On Industry Applications*, *27*(2).

Wang, Y., & Forssberg, E. (2005). Dry comminution and liberation with microwave assistance. *Scandinavian Journal of Metallurgy*, *34*(1).

Wills, B. A. (1990). Comminution in the minerals industry - An overview. *Minerals Engineering*, *3*(1–2).

Wills, Barry A., & Finch, J. A. (2016a). Chapter 5 – Comminution. *Wills' Mineral Processing Technology*.

Wills, Barry A., & Finch, J. A. (2016b). Introduction. *Wills' Mineral Processing Technology*, 1–27.

Wills, Barry A., Finch, J. A., Wills, B. A., & Finch, J. A. (2016a). Chapter 4 – Particle Size Analysis. *Wills' Mineral Processing Technology*.

Wills, Barry A., Finch, J. A., Wills, B. A., & Finch, J. A. (2016b). Chapter 6 – Crushers. *Wills' Mineral Processing Technology*.

Wilson, M. G. C., & Anhaeusser, C. R. (1998). The mineral resources of South Africa. Sixth edition. In *The mineral resources of South Africa. Sixth edition*.

Yates, A. (1918). Effect of heating and quenching Cornish tin ores before crushing. *Transactions of the Institute of Mining and Metallurgy*.

Appendix

Appendix A: Specific Comminution Energy Calculation Table for Treated Sample

	Recorded data					Net power	Specific comminution energy			Crushing time	Nontreated		Relative		MW impact (%)	
	Time (s)	Current (A)	Power (W)	Voltage (V)	Power Factor	W	Joules	kW.hr_Net	kW.hr/t	Actual time (s)	Net Power (W)	Esc (k.W.hr/t)	Power (W)	Esc (k.W.hr/t)	Power (W)	Esc (k.W.hr/t)
1	64		73.5			0	0	0.000000	0.000	0	0	0	0	0	0	0
2	65	3.193	303	119	0.8	229.5	188.25	0.000032	0.064	1	60.74	0.0168722	3.7784	3.793574	-277.84	-279.3574
3	66	4.79	476	118	0.84	402.5	577.75	0.000120	0.240	2	189.88	0.0864889	2.11976	2.7780057	-111.976	-177.80057
4	67	4.79	476	118	0.84	402.5	1053.75	0.000231	0.465	3	252.58	0.2093944	1.593555	2.2196184	-59.3555	-121.96184
5	68	3.929	390	119	0.84	316.5	1486.75	0.000331	0.665	4	259.04	0.3515111	1.221819	1.8926858	-22.1819	-89.26858
6	69	4.325	438	118	0.84	364.5	1900.75	0.000426	0.855	5	279.04	0.5009778	1.306264	1.7071146	-30.6264	-70.711457
7	70	4.273	420	118	0.83	346.5	2329.75	0.000525	1.054	6	276.92	0.6554111	1.251264	1.607418	-25.1264	-60.741803
8	71	4.282	426	118	0.82	352.5	2752.75	0.000622	1.248	7	307.72	0.8178111	1.145522	1.5265947	-14.5522	-52.659467
9	72	4.282	426	118	0.84	352.5	3178.75	0.000720	1.445	8	283.12	0.9819333	1.245055	1.4716741	-24.5055	-47.167415
10	73	3.444	344	119	0.84	270.5	3563.75	0.000806	1.619	9	301.32	1.1442778	0.897717	1.4147233	10.22833	-41.472332
11	74	3.208	318	119	0.84	244.5	3894.75	0.000878	1.762	10	283.72	1.3067889	0.861765	1.3487003	13.82349	-34.870027
12	75	3.151	315	119	0.84	241.5	4211.25	0.000945	1.898	11	231.52	1.4499111	1.043106	1.3090518	-4.31064	-30.905177
13	76	3.151	315	119	0.83	241.5	4526.25	0.001012	2.033	12	225.32	1.5768111	1.071809	1.2891298	-7.1809	-28.91298
14	77	2.674	263	119	0.83	189.5	4815.25	0.001072	2.153	13	200.52	1.6951	0.860263	1.3296423	13.97367	-32.964227
15	78	2.468	246	119	0.84	172.5	5069.75	0.001122	2.254	14	189.52	1.8034444	0.762453	1.2987846	23.75475	-29.878457
16	79	2.186	218	119	0.84	144.5	5301.75	0.001166	2.342	15	193.72	1.9099	0.745922	1.2685931	25.40781	-26.859311
17	80	2.186	218	120	0.82	144.5	5519.75	0.001207	2.423	16	178.32	2.0132444	0.372925	1.232703	62.70749	-23.270301
18	81	1.429	140	120	0.82	66.5	5698.75	0.001236	2.482	17	156.92	2.1063667	0.302702	1.1932995	69.7298	-19.329952
19	82	1.262	121	120	0.81	47.5	5829.25	0.001252	2.514	18	184.12	2.2011	0.214534	1.1529644	78.5466	-15.296445
20	83	1.171	113	120	0.81	39.5	5946.25	0.001264	2.538	19	179.92	2.3022222	0.064473	1.1085122	93.55269	-10.851223
21	84	0.894	85.1	120	0.79	11.6	6045.3	0.001271	2.552	20	144.72	2.3924	0	0	100	100
22						0	0	0.000000	0.000	21	128.72	2.4683556	0	0	100	100
23						0	0	0.000000	0.000	22	117.12	2.5366444	0	0	100	100
24						0	0	0.000000	0.000	23	103.12	2.5978222	0	0	100	100
25						0	0	0.000000	0.000	24	100.12	2.6542778	0	0	100	100
26						0	0	0.000000	0.000	25	56.72	2.6978444	0	0	100	100
27						0	0	0.000000	0.000	26	49.9	2.7274611	0	0	100	100
28						0	0	0.000000	0.000	27	49.66666667	2.7551185	0	0	100	100
29						0	0	0.000000	0.000	28	34.5	2.7784981	0	0	100	100

Appendix B: Heat absorbed and HOME % Calculations Method

The initial temperature of the rock sample (T_{R1}) was measured using the IR camera. Then, the initial temperature of water (T_{W1}) inside the calorimeter was measured using the thermometer. The final temperature of water (T_{W2}) and rock samples (T_{R2}) after microwave treatment was the same as the rock samples were immersed in the water and reached the state of equilibrium. Next, the surface temperature of rock samples after microwave treatment was measured with an IR camera to check the maximum temperature of the samples. The mass of the sample (m_R) was around 500 g, and the mass of water (m_W) was 1000 g. The value of specific heat capacity ($C_{p,R}$) of HK kimberlite is 0.94 kJ/kg.K (Deyab et al., 2021), and that of water ($C_{P,W}$) is 4.72 kJ/kg.K. These values were used to calculate the heat energy (Q_{total}) in the calorimeter.

$$Q_{total} = Q_R + Q_W \quad (27)$$

$$Q_R = m_R * C_{P,R} * (T_{R2} - T_{R1}) \quad (28)$$

$$Q_W = m_W * C_{P,W} * (T_{W2} - T_{W1}) \quad (29)$$

The total heat absorbed is then used to calculate the HOME % by using the following relation

$$\text{HOME } \% = \frac{Q_{total}}{\text{MW Input}} = \frac{Q_{total}}{\text{Power} * \text{Exposure time}} \quad (30)$$

Appendix C: GGS and RR model Plots and PSD Method for Samples

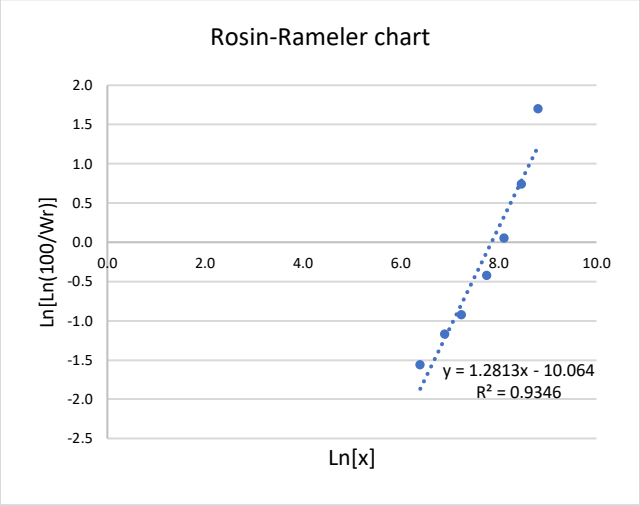

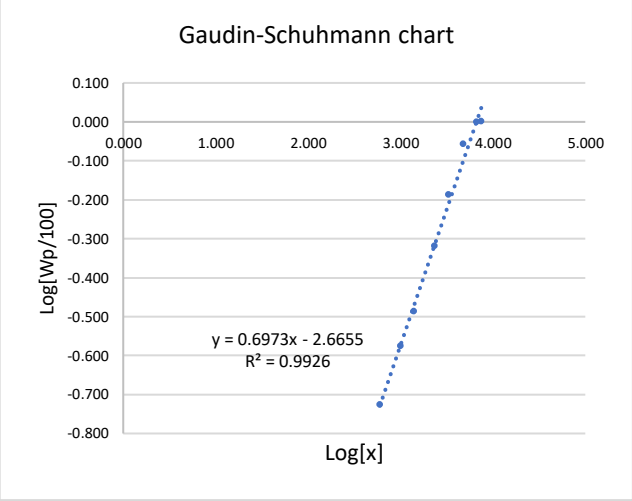

Rosin-Rameler PSD Model							
X (µm)	**lnX**	**Wr (%)**	**100/Wr**	**Ln[100/Wr]**	**Ln[Ln(100/Wr)]**	**Wr Pred (%)**	**Error (%)**
6700	8.810	0.430	232.514	5.449	1.695	3.334	675.14
4750	8.466	12.364	8.088	2.090	0.737	11.205	-9.38
3350	8.117	35.168	2.843	1.045	0.044	24.677	-29.83
2360	7.766	52.087	1.920	0.652	-0.427	40.931	-21.42
1400	7.244	67.482	1.482	0.393	-0.933	63.285	-6.22
1000	6.908	73.462	1.361	0.308	-1.176	74.283	1.12
600	6.397	81.251	1.231	0.208	-1.572	85.684	5.46
1	0.000	100.000	1.000	0.000			

Gaudin-Schuhmann PSD Model						
X (µm)	**LogX**	**Wp (%)**	**Wp/100**	**Log[Wp/100]**	**Wp Pred (%)**	**Error (%)**
7500	3.875	100.000	1.000	0.000	108.767	6.42
6700	3.826	99.570	0.996	-0.002	100.541	-0.94
4750	3.677	87.636	0.876	-0.057	79.101	-9.25
3350	3.525	64.832	0.648	-0.188	62.007	-1.53
2360	3.373	47.913	0.479	-0.320	48.569	3.70
1400	3.146	32.518	0.325	-0.488	33.747	4.81
1000	3.000	26.538	0.265	-0.576	26.689	0.68
600	2.778	18.749	0.187	-0.727	18.692	0.68